WAVELENGTH MODULATION SPECTROSCOPIC CHEMICAL SENSING USING A PIEZO-ELECTRIC TUNABLE FIBER BRAGG GRATING LASER

by

Michael Buric

B.S. in Electrical Engineering, University of Pittsburgh, 2002

Submitted to the Graduate Faculty of

The School of Engineering in partial fulfillment

of the requirements for the degree of

Master of Science in Electrical Engineering

University of Pittsburgh

2005

UNIVERSITY OF PITTSBURGH

SCHOOL OF ENGINEERING

This thesis was presented

by

Michael Buric

It was defended on

September 6, 2005

and approved by

Joel Falk, PhD, Professor, Electrical and Computer Engineering Department

Dietrich Langer, PhD, Professor, Electrical and Computer Engineering Department

Thesis Advisor: Kevin Chen, PhD, Professor, Electrical and Computer Engineering Department

ABSTRACT

WAVELENGTH MODULATION SPECTROSCOPIC CHEMICAL SENSING USING A PIEZO-ELECTRIC TUNABLE FIBER BRAGG GRATING LASER

Michael Buric, M.S.

University of Pittsburgh, 2005

Real time gas sensing is paramount to numerous applications in industry as well as in the consumer sector. Many gas sensing applications such as fossil energy production require low-cost, multi-species sensors that are able to operate in high-temperature, high-pollution environments under the presence of strong electromagnetic fields. Optical remote gas sensing using tunable lasers is regarded as the best sensing technology for hostile environments. However, optical technology often suffers from high component and operational costs.

In this thesis, a tunable external-cavity fiber Bragg grating (FBG) diode laser was developed for spectroscopic chemical sensing. Although FBG lasers have been reported upon, previous works have focused primarily on telecommunications applications. This thesis reports the first application, to our best knowledge, of an FBG laser in chemical sensing. This fiber Bragg grating laser was comprised of an InGaAs/InP ridge-waveguide laser diode coupled to a length of SM-28 fiber bearing an FBG. The FBG is stretched via a piezo-electric actuator to allow rapid fine tuning of the output wavelength of the laser. This tunable external-cavity semiconductor laser was demonstrated with over 10 nm of tuning range. The measured spectral width of the laser was instrument-limited at less than 50 pm over the entire tuning range. The application of such low-cost tunable FBG lasers to spectroscopic chemical sensing was demonstrated in acetylene (C_2H_2) gas with a wavelength modulation spectroscopy technique. Both static and wavelength modulation absorption spectra of acetylene gas were observed by the

tunable laser in acetylene partial pressures from 0.1 mbar to 100 mbar; the lowest detectable pressure being limited by the ultimate vacuum pressure and length of our gas cell.

In terms of other optical gas sensing devices such as Distributed FeedBack lasers, FBG lasers offer much lower manufacturing costs and better temperature stability (13pm/ºK) over DFB lasers (>100 pm/ºK). The low manufacturing cost, good temperature stability, wide tuning range, and high output power make FBG lasers excellent candidates for the application of chemical sensing in the near IR band.

TABLE OF CONTENTS

LIST OF TABLES

LIST OF FIGURES

ACKNOWLEDGEMENTS

I would certainly be remiss to neglect to mention a number of people who made my research and course of study a reality. Firstly, I would like to thank Dr. Kevin Chen and the Pittsburgh Digital Greenhouse for funding the entirety of this work. More importantly, Dr. Chen has taught me more than I ever thought possible in the field of optical electronics. Without his astute guidance, none of this would have been possible. Secondly, I would like to thank Dr. Joel Falk for his unending assistance in the realm of theory. I feel that his level of analysis makes him a true man of science without which I would undoubtedly be lost. I would also like to thank Dr. Dietrich Langer under whom I conducted my first optical experiment as a Senior Design Project. He is surely the reason for which I study in the field of optics and electronics today.

Certainly, a great deal of credit is due to those around me from whom I derive a great deal of emotional support. I would therefore like to thank my fellow graduate research assistants, Lucas Cashdollar, Ben McMillen, Chuck Jewart, and Zsolt Poole who are a constant aid to my efforts. Special thanks go to Mr. Brett Bernardo for furnishing some of the CAD drawings following. I would also like to thank Sandy Weisberg and Angela Ellis for their unending guidance throughout my academic career. Finally, the most credit is surely due to my Mom, my brother, my best friend Elizabeth, and the gentlemen of Akrasia L.L.C. just for being there.

1.0 INTRODUCTION

1.1 MOTIVATION

Fiber Bragg grating lasers have been demonstrated in numerous incarnations in the past several years. Currently a relatively new technology; they are proving invaluable to the telecommunications industry. To date, such technology is rarely utilized outside telecom. There are, however, a myriad of possible applications for such a precise and versatile light source. One such application is that of a spectroscopic gas sensing device. Currently, the author is unaware of any FBG laser based gas sensing device despite exhaustive searches through relevant literature.

The principle behind spectroscopic sensing is relatively simple. Every existent chemical compound in the universe exhibits a distinct light absorption pattern. This pattern is produced as incident light of specific wavelengths is absorbed and transformed into energy in the compound. This phenomenon results in the colors of everyday objects evidenced by our limited visual faculties absorbing those wavelengths of light that are reflected by the objects. Such absorptive transitions are not merely confined to the miniscule range of the visual spectrum. Absorptions occur over the entire electromagnetic spectrum. In fact, some of the most detailed and distinct absorptions occur in many chemical compounds over the infrared spectrum.

The process of spectroscopic sensing is most simply the quantification of the absorption associated with a given chemical compound. Once the absorption spectrum of a chemical is known, the absorption of a test gas may be compared to the known spectrum in order to determine the presence or absence therein of the test chemical in question. Most absorptive transitions absorb a very narrow band of wavelengths of incident light. Fortunately for analysis, it is often possible to distinguish a number of different chemicals from a single absorption line in its spectrum because it is distinct from those absorptions of other possibly present species, and significantly far enough away from other absorption lines in its own absorption spectrum. It should then be readily apparent that the necessary tool for spectroscopic chemical sensing is an extremely monochromatic light source that can be quickly tuned over a range of wavelengths.

Modern spectroscopic chemical sensing utilizes a number of different types of laser sources in different applications. The end goal is obviously to be able to tune the laser source to a number of different absorption lines. The laser source is then shone through a particular test gas while remaining light is recovered and measured in intensity. This intensity measurement then may be used to calculate the relative concentration of the species in question. Temperature-tuned distributed feedback (DFB) lasers, multi-section distributed Bragg reflector lasers, external cavity lasers, optically pumped vertical cavity surface emitting lasers (VCELs), and MEMS-based VCSELs have all been previously utilized for various sensing applications. These laser sources, however, usually suffer from low output power, slow tuning speed, a narrow tuning range, and high manufacturing costs. The application herein purports excellent utilization of the inherent properties of a tunable external cavity FBG laser.

Fiber Bragg gratings were first developed in the 1970's. In the most simplistic of terms, an FBG is an optical fiber with a core index of refraction that has been periodically modulated

over some portion of its length. Such a Bragg structure possesses the inherent property of being reflective at a particular wavelength of light due to constructive and destructive interference formed as light passes through the changing index in the fiber. It has been extensively shown that the central wavelength reflected by the FBG can be "tuned" up or down by a number of means including piezo-transducers, Peltier devices, light-heated electrically resistive coatings, and mechanical bending devices. Each of these methods essentially changes the length of the grating, in addition to the index of refraction in the fiber due to induced strain. Because of this tuneability property, tuneable FBGs are often used as filters in telecommunication systems or as part of multiplexers or de-multiplexers.

Fiber Bragg gratings are simple to fabricate, and are thus readily available in the consumer optics market. By coupling a fiber Bragg grating to a readily available laser diode, it has been shown that one can quite simply construct an external cavity FBG laser. By tuning the FBG as previously described, we can tune the output wavelength of the laser. Because of recent innovations in FBG production, it is also possible to produce an FBG laser with up to about 90nm of tuning range. This range far exceeds the range of wavelength possible using VCELs, because VCELs have traditionally been purely cavity thermally tuned devices. It should also be noted that FBG lasers usually tune more rapidly than VCELs and other thermally tuned devices due to the specific heat of the lasing material requiring that the medium take some time to stabilize in temperature.

The work to be described herein was motivated by the realization that existent optical technologies could in fact be applied to the spectroscopic sensing problem in order to realize an inexpensive and highly accurate system. The prospect of using FBG lasers for chemical sensing seems to be an intrinsically appropriate application. On one hand, we have an extremely

versatile light source with excellent fast tuneability, narrow wavelength output, good stability, and fairly low production costs. On the other, we have an application requiring just such a device. We intend to show that the application of such a laser to spectroscopic chemical sensing results in an extremely effective and appropriate contrivance.

1.2THESIS ORGANIZATION

Chapter 2 contains an assortment of background information pertinent to this thesis. Included is a brief theory of Bragg gratings along with a summary of grating fabrication techniques. Also detailed are the schemes of operation for various types of lasers commonly utilized for chemical sensing. These include temperature-tuned distributed feedback (DFB) lasers, vertical cavity surface emitting lasers (VCELs), and of course external cavity FBG lasers. Also found in this section is a treatise on chemical absorption with derivations for the strength of chemical absorption lines and other absorption mathematics relevant to this discussion. Finally, the wavelength modulation second-harmonic measurement technique implemented for species concentration measurement is detailed.

Chapter 3 details the experimental setup utilized in the research herein. It begins with a detailed description of the fabrication of the FBG laser used for sensing, along with relevant output characteristics of the device. Details regarding the tunability of the device are also presented. Finally, the test-bench setup for the measurement of acetylene gas absorption is discussed.

Chapter 4 contains experimental results obtained with the tuneable FBG chemical sensing setup. Attention is given to the operational characteristics of the device. Careful comparison is made to baseline absorption data, and considerations are made regarding the significance of results obtained herein.

Chapter 5 contains a series of conclusions drawn from the data presented in Chapter 4, as well as a summary of the work presented in this thesis. The chapter also contains a section on possible future work that would expand on the experimentation presented here and foster the completion of an inexpensive hand-held chemical sensing unit suitable for a number of industrial and consumer applications.

2.0 BACKGROUND INFORMATION

2.1 FBG THEORY AND CHARACTERISTICS

Fiber Bragg Gratings were first introduced to industry in the 1980's after K.O. Hill and associates discovered the first known fiber grating fabrication technique in 1978 (1). Since then, FBGs have found their way into numerous optical telecommunications devices. Because of their central role in the operation of the tunable FBG Laser presented herein, we will briefly examine the physical principles governing the operation of an FBG. A few of the common techniques implemented in the construction of FBGs will also be detailed. Such an examination will allow the reader to better comprehend the operation of the FBG laser and its application to chemical sensing.

A Fiber Bragg Grating is, most simply, a periodic change in the index of refraction of the core of an optical fiber. Light propagating down the length of a fiber containing a Bragg Grating will reflect back only at one particular wavelength known as the Bragg Wavelength (λ_B). Light at other wavelengths will pass through the fiber with little attenuation. The Bragg wavelength is determined by both the period of the index change in the fiber (Λ), as well as the effective index of refraction of the fiber's core (n_{eff}). Thus, the Bragg or reflecting wavelength is found as:

$$\lambda_B = 2n_{eff}\Lambda \tag{2}$$

Figure 1 is a basic diagrammatic interpretation of the Bragg reflection concept as applied to optical fiber. The reflection and transmittance spectra shown therein should be carefully reviewed. It is important to note that although reflection occurs at one particular wavelength, that same reflection spectrum has a finite width ($\Delta\lambda$) usually encompassing anywhere from .01nm to .2 nm based upon the realized index change in a particular grating as well as the overall grating length. This width is referred to as the bandwidth of the grating, and will play an important role in the characteristics of the FBG laser. It is also important to note that the reflection peak has a finite height. The height of the reflection peak indicates what portion of light at the Bragg wavelength is reflected back down the fiber. The reflectivity of an FBG is usually denoted as a percentage of reflected intensity verses transmitted intensity at the Bragg wavelength. The reflectivity of a given FBG may be altered by varying the length (number of grates or index changes) and the intensity of the index change in the grating. The reflectivity of the FBG will also determine the output characteristics of the FBG laser.

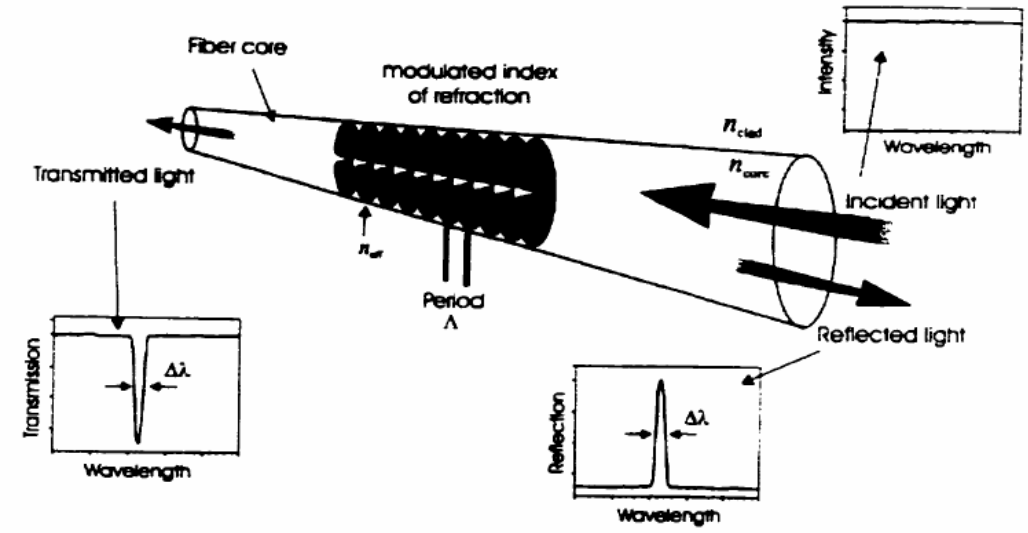

Figure 1 – Operation of an FBG (2)

By applying the simple principles governing the variation in Bragg reflection spectra, engineers are currently using FBGs to construct filters, multiplexers, de-multiplexers, sensors, and other devices for telecommunications. In the realm of grating fabrication, several techniques tailored to specific types of FBGs have emerged to produce these fiber devices on industrial scale. The first of these techniques, which was actually stumbled upon accidentally by Hill et. al, is the internal writing technique. Relatively poor gratings resulted from this technique, initiating the development of interferometric fabrication, phase masking techniques, and finally point-by-point fabrication.

In 1978 K.O. Hill et. al. discovered that coherent standing waves from an Argon/Ion laser in a germanium doped silica optical fiber produce a periodic index change with the same period as the standing wave. Discoveries therein were two-fold. Firstly, standard germanium doped silica telecommunications fiber can actually have its index of refraction

altered via incident light of the correct wavelength. Secondly, a Bragg reflector, which had only previously been constructed with multiple layers of different index material, could be created inside an optical fiber utilizing this newfound photosensitivity effect. Later, it was fairly conclusively determined that the photosensitivity effect is caused by rearrangement of the germanium bonding structure in the optical fiber upon light exposure at the correct wavelength (157, 193, ~250 or 260 nm) (8). Although a complicated setup was required to produce standing waves in optical fiber, and alterations to the characteristics of the inscribed grating were almost impossible, it was shown that inscription of optical fiber with a Bragg reflector was possible (1).

Hill et. al. later showed that the index of refraction in optical fiber could also be altered via exposure to high energy pulses from a KrF laser normal to the length of the fiber. Such finding led to both the phase mask inscription technique as well as the point-by point inscription technique. In the former, a high energy coherent KrF laser is used to illuminate a silica phase mask. The mask is constructed usually via ion beam etching or some other micro-imprinting technique. Once inscribed with alternating opaque and translucent lines, the mask may be utilized to relegate the intensity of the KrF laser incident upon the photosensitive optical fiber. In such a way, a grating may be manufactured in a matter of seconds or minutes with little alignment after initial laser and mask setup (6,9,13).

Point-by-point grating inscription is very similar to the phase mask technique described above, save that it offers a great deal of flexibility with the only real drawback being production time. In a point-to-point writing setup, a KrF laser is culminated in a tiny single slit. The fiber itself is mounted upon a precise (usually interferometrically controlled with a separate control light source) mechanical stage that allows translation along the fiber length relative to the laser output slit. A single pulse from the laser is used to photosensitize one grate of the FBG

before the fiber-stage is translated some length for inscription of the next grate. In such a manner, FBGs with any arbitrary Bragg wavelength and grating length may be fabricated without the need for a number of different expensive phase masks. Unfortunately, as one might imagine, the time required to write a grating in this fashion, including the continuous exposure and translation of the fiber, is much longer than that of a phase mask procedure requiring only a single exposure. The point-by-point writing technique could prove invaluable to the experiments described subsequently herein due to the necessity of FBGs with fairly uncommon Bragg wavelengths.

The final technique to be detailed for the inscription of FBGs is the interferometric technique. Meltz et. al. had first shown that a holographic interferometer could be utilized to inscribe photosensitive fiber. In such a technique, a single beam from a KrF laser is split into two beams and subsequently re-joined at an angle (α) in order to produce a beam interference pattern of light and dark fringes. Such an interference pattern may effectively inscribe an FBG. In addition, changing the wavelength of the laser source will change the distance between fringes, and thus the Bragg wavelength of the grating. Although hailed to be an effective technique, interferrometric writing is used much more seldom than phase mask or point-by-point writing (7).

2.2 FBG TUNING

The primary purpose for detailing the characteristics of FBGs is to provide the basis of understanding necessary to discuss the external cavity FBG laser. It will also be necessary to

review several common methods of tuning the characteristics of FBGs in order to begin discussion on tuning the FBG laser itself. Herein, we will discuss FBG tuning via mechanical stretching, bending, and heating.

Initially, we specified the Bragg wavelength as being determined by:

$$\lambda_B = 2n_{eff}\Lambda$$

where Λ is the period of index modulation in the optical fiber. The period (Λ) can be calculated for a given grating by:

$$\Lambda = L/n$$

where L is the total length of the grating and n is the number of sequential index changes in that length for a linearly indexed common Bragg reflector. It should be fairly obvious that if the length of the fiber is increased by mechanical stretching, the Bragg wavelength will then shift towards longer wavelengths. The less obvious result of stretching an FBG is that the index of refraction of the fiber also changes under strain.

The physics behind the stretching and straining of materials, including optical fiber, is very well established (26). If we are to shift the Bragg wavelength of an FBG via mechanical stretching, we can refer to the physical properties of the optical fiber material itself in order to attain information regarding the resultant changes in the material (5). When stretching a fiber, the Bragg wavelength will be changed due solely to change in its index of refraction as:

$$\Delta\lambda_B = \lambda_B(1 - p_e)\varepsilon_z$$

The applied strain (ε_z) is found by:

$$\varepsilon_z = \Delta L / L$$

where ΔL is the change in length of the grating and L is the original length of the grating. The strain-optic constant (p_e) is usually about .22 for silica fiber material. In general, the wavelength

change due to the actual change in periodic length will be only about 6% of the change brought about by the index of refraction change in the fiber. In performing mechanical stretching of an FBG, one must take care not to exceed the Deformation Strain of the fiber. This value is, however, usually greater than 3500 uStrain (.35% length change). In fact, the large yield strain of silica fibers makes them ideal for use in strain gauges commonly used in structural strain sensing (3,20).

Another effective method for wavelength tuning of an FBG is to change the temperature of the grating. Again, most of the effects resultant from temperature changes in silica fiber are due to changes in the refractive index in the fiber, and not simply thermal expansion. The Bragg wavelength change resulting from a given temperature change is given by:

$$\Delta\lambda_B = \lambda_B *(\alpha+\xi)\, \Delta T$$

where α is the thermal expansion coefficient and ξ is the thermo optic coefficient. Aggregating both equations for wavelength changes due to temperature and strain, we find that:

$\Delta\lambda_B = \lambda_B *((\alpha+\xi)\, \Delta T + (1 - p_e)\, \varepsilon_z)$

Values for standard silica fiber would result in:

$\Delta\lambda_B = \lambda_B * (8.85\times10\text{-}6\, \Delta T + 0.78\times10\text{-}6\, \varepsilon_z)$

Thus, a one-Kelvin change in temperature would cause about the same wavelength shift as a 10 uStrain stretch (6).

Another effective way to alter the transmission properties of an FBG is via bending of the inscribed grating. In such a setup, an FBG is bonded to an elastic beam above the center axis of the beam as shown in Figure 2. Subsequent bending of the beam induces compressive strain on the FBG, altering its index of refraction in much the same manner as elastic stretching. The advantage to utilizing bending is that it is compressive in nature, and much higher strains can be

introduced with a decreased possibility grating failure. Also, the encasing beam serves as a stabilizing medium to equalize the strain and add strength to the fiber structure. Using such a bending scheme, the Bragg wavelength has been shown to shift up to 90nm without permanently deforming the FBG. The equation governing the change in Bragg wavelength may again be given as:

$$\Delta\lambda_B = \lambda_B(1 - p_e)\varepsilon_z$$

In this case, the strain (ε_z) may be found as:

$$\varepsilon_z = d*\theta/L$$

where d is the FBGs distance from the center of the bending beam, L is the length of the beam, and θ is the arc-angle that the beam is bent to. The previous equation shows us that a great deal of strain can in fact be applied via the bending method as opposed to elastic stretching. Unfortunately, beam bending is a relatively slow means of Bragg wavelength adjustment as opposed to stretching. Because an additional mechanical material (the beam) must be stressed, it requires some time to deform and relax in the tuning process. Such relaxation time slows the tuning speed of a bending setup (5).

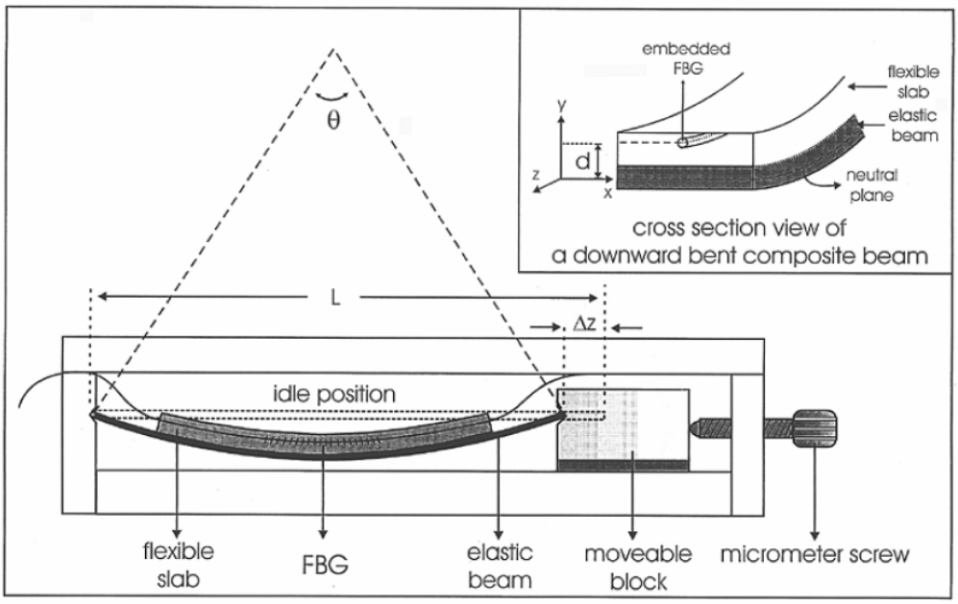

Figure 2 - FBG Bending to alter the Bragg Wavelength (5)

2.3 THE FBG LASER

Now that some understanding has been gained in the realm of Fiber Bragg Gratings, it should next be logical to detail the means by which an external cavity laser is constructed using an FBG. In detailing the operation of an FBG laser, we will first briefly review the operation of a regular single cavity laser, then we will expound upon the concept of an external cavity laser using an FBG as a reflector. The physical relevance of Vernier tuning will also be addressed.

The concept of stimulated emission was first dreamed up by Albert Einstein in 1917. Since then, researchers have devised a number of clever means by which to coax a material into giving up its photons. In a standard laser cavity, light reflects between a low-loss reflector and a

semi-transparent exit reflector. Between the reflectors, a gain medium is required to emit additional photons in the amplification of the laser beam. The resultant resonator mode spacing realtes to the speed of light in the gain medium (c_o) and the distance between the cavity reflectors (d) as:

$$\nu_f = c_o / 2d \text{ where } c_o = c*n$$

This is because the resonator cavity only sustains frequencies that correspond to a round-trip optical phase shift that is a multiple of 2π, where that same phase shift (k) is determined by:

$$k = 2 \pi \nu / c_o$$

Figure 3 is a diagram of the cavity modes in a standard internal cavity laser which are equally spaced as per the above equation.

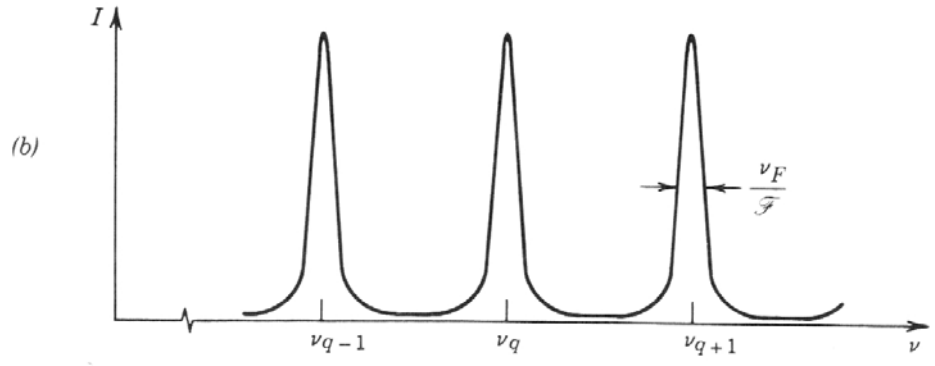

Figure 3 – Internal Cavity Laser Resonator Modes (23)

An external cavity FBG laser is somewhat more complicated. Therein, a gain medium with a single "back" reflector is utilized as a light amplification source. The gain medium is often an Optically Emitting Semiconductor mounted in an on-chip package with a single highly reflective coating at the non-emissive end. Because the index of refraction associated with the

gain medium is often much higher than that of the surrounding atmosphere, as well as that of most silica waveguide materials, there are subsequent reflections back into the cavity at the gain medium/air interface. These reflections serve to initiate some inherent cavity modes despite the lack of a deliberately installed exit reflector. Energy output amplitude is, however, distributed amongst these modes following the generally Lorentzian line-shape of the gain medium's gain coefficient. Figure 4 shows a common output mode structure of a gain medium with a single back reflector terminated in atmosphere. With current semiconductor technologies producing relatively short cavity sizes and broad gain coefficients, it is possible to achieve a large number of closely spaced modes over a large wavelength range.

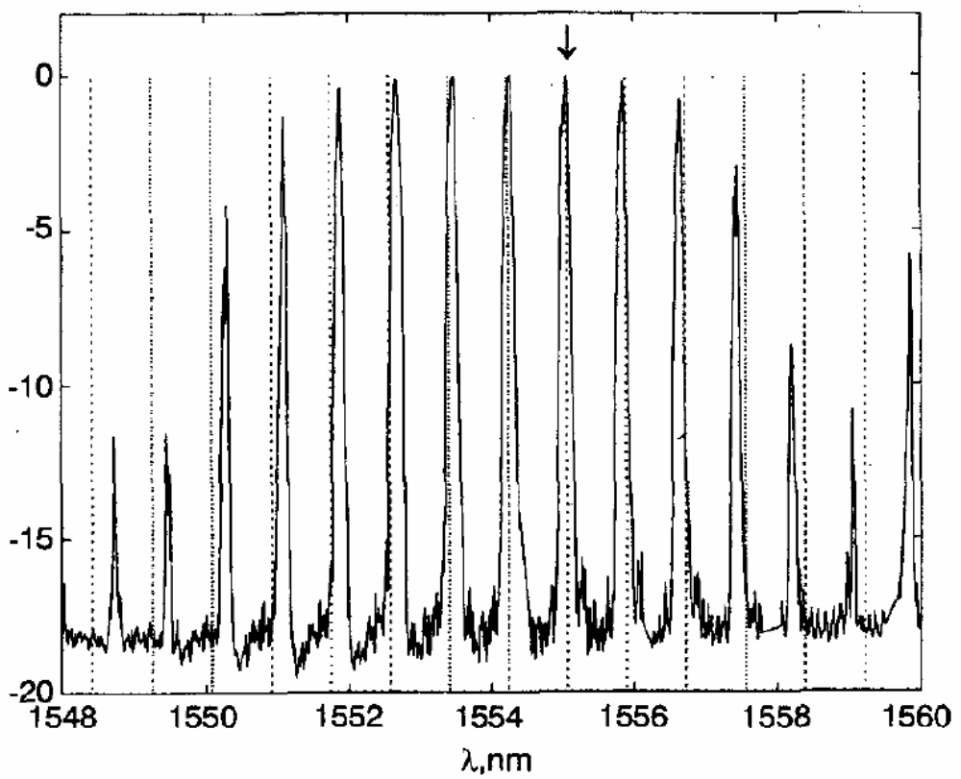

Figure 4 - Mode Structure of a Generic Semiconductor Gain Medium (25)

The introduction of an FBG coupled to the output of such a single reflector cavity produces some interesting results. Such a setup is diagrammed in Figure 5. In essence, the Bragg grating is going to serve as the output reflector for the laser, thus replacing the non-existent output cavity reflector. Photons will then be forced to make the round trip amplification circuit between the reflective Bragg grating inside coupled optical fiber and the back reflector at the other end of the gain medium. Therein, amplification occurs only inside the short section of gain medium material, while some amount of optical loss occurs in the fiber section of the circuit. If the laser oscillation condition is met, or:

$$\gamma_o > \alpha_r$$

(where γ_o and α_r are the small signal gain coefficient and total system loss coefficients respectively), then lasing may occur.

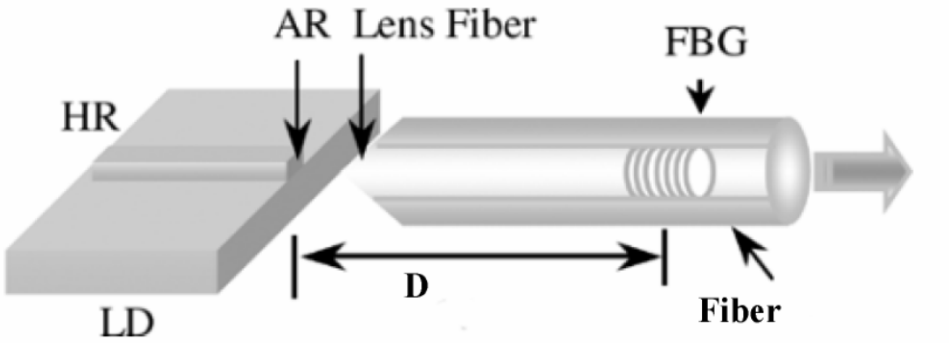

Figure 5 – FBG Laser Basic Diagram (18)

In order for the laser resonance conditions to be satisfied, several things must happen. First, adequate coupling must exist between the gain medium and the optical fiber so that overall laser gain is not extensively diminished. Secondly, the amount of reflectivity at the

fiber/semiconductor interface must not be excessive or else lasing may occur only inside the cavity, and not externally as is the goal of constructing an external cavity laser. This may be accounted for by the application of an anti-reflective coating between the gain medium and the affixed optical fiber. Finally and most importantly, in order for lasing to occur, the light output from the gain medium must be reflected by the Bragg grating. If we observe the reflection spectrum together with the output spectrum of the light source as in Figure 6, then we will note that one of the inherent cavity modes coincides with the Bragg wavelength of the FBG. This is the wavelength that undergoes amplification and will also be the output wavelength emitted from the laser. As this reflection peak coincides with one of the resonant cavity modes, energy will be effectively "leeched" from the other modes, causing them to diminish in size, or disappear entirely.

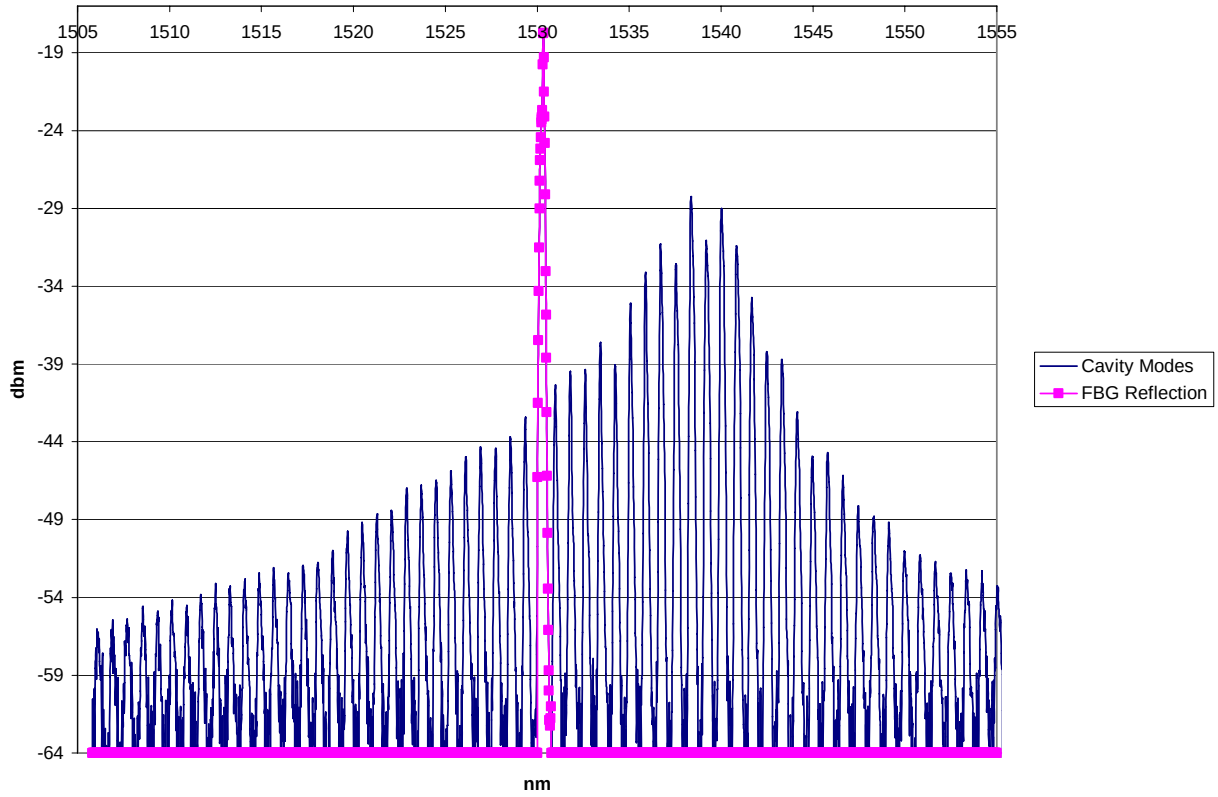

Figure 6 – Inherent Cavity Modes and FBG

2.4 FBG LASER TUNING

The primary purpose behind constructing an external cavity FBG laser is usually the ease with which one may wavelength-tune such a device. Previously, we examined the necessary conditions for lasing with an FBG in indicating that one of the resonant cavity modes must align with the Bragg wavelength of the FBG. We also examined the ability of an FBG to be

wavelength-tuned via stretching, heating, or bending. If we simultaneously apply these two concepts, we can see how one might tune an FBG laser. Figure 7 shows an FBG reflection spectrum as it is shifted via mechanical stretching. As the Bragg wavelength aligns with one of the natural cavity modes, lasing may occur at any one of these modes. This is commonly known as "step" or "Vernier" tuning (25).

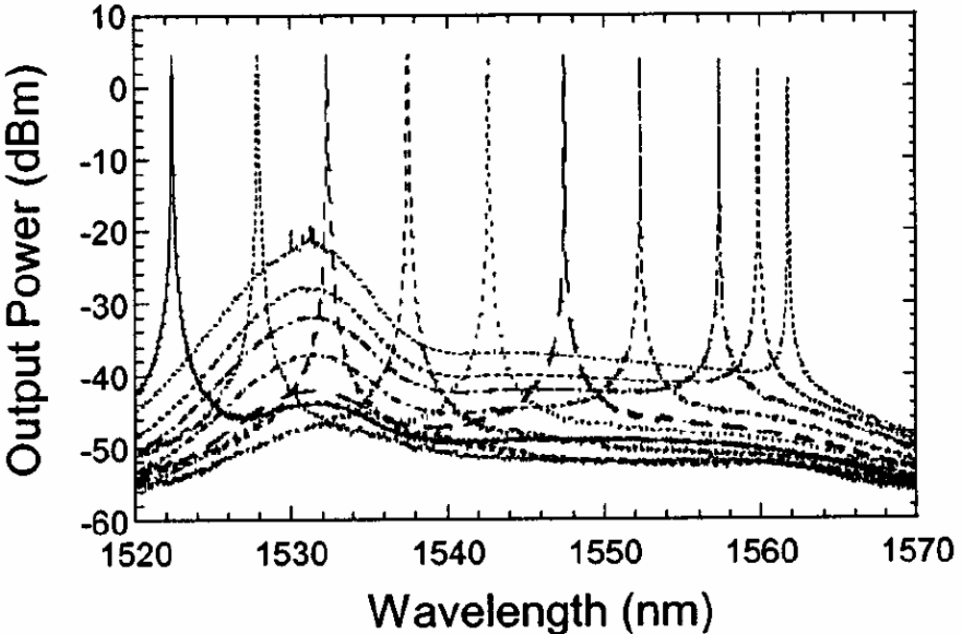

Figure 7 – Shifting FBG Reflection Spectrum for Vernier Tuning (25)

There are several other means by which one may tune the FBG laser in addition to simply stretching or bending the Bragg grating. Previously, we detailed the condition for resonance inside the gain medium as being dependant upon the length of the cavity and the index of the gain medium. Most known gain mediums possess positive temperature coefficients, meaning that they expand when heated. In the case of a semiconductor medium, as current passes through the material, photons are emitted in addition to some amount of heat being generated, thus

expanding the cavity and making the overall cavity length larger. A longer cavity length will result in the shifting of all resonant cavity modes towards toward longer wavelengths. Several added beneficiary properties result from this phenomenon. Firstly, one may apply an FBG with a relatively wide reflection line width. Provided the cavity line widths are still fairly narrow, we may then simply use the cavity temperature (or injection current in a semiconductor application) to tune the laser output over the wavelength range allowed by the reflection spectrum evident in the grating.

We may also choose to simultaneously stretch the FBG and add injection current to the cavity, thus increasing the Bragg wavelength and the cavity mode wavelengths at the same time. This allows continuous tuning over some significant range of wavelengths. Finally, we can choose to utilize some combination of temperature tuning and Vernier tuning by which the largest possible range of output wavelengths may be realized. In such a system, the FBG would first be tuned to any desired wavelength over the cavity output spectrum. Then, the cavity temperature would be adjusted to align the closest natural cavity mode to the tuned Bragg wavelength, thus lasing at that wavelength.

In general, FBG lasers have been developed as extremely versatile and utilitarian optical sources. We have seen that wavelength tuning with an FBG laser is relatively simple, in being that a number of fiber tuning methods exist. We have also noted that construction of FBG lasers may be accomplished with little manufacturing cost resultant from the abundance of cheap semiconductors and inexpensive optical fiber. We will subsequently embark upon the basis with which we may apply the tunable FBG laser to a chemical sensing system, thus producing a low-cost device utilizing the beneficial characteristics of the FBG laser.

2.5 OTHER TYPES OF SENSING LASERS

Now that the reader has been thoroughly familiarized with the external cavity FBG laser, we may begin to introduce a few of the other common lasing devices used in chemical sensing applications. We will examine both temperature-tuned distributed feedback (DFB) lasers and vertical cavity surface emitting lasers (VCSELs) because they propone two of the best small-scale alternative strategies for sensing applications. Understanding these types of devices will better impart the rationalization with which an FBG based laser was chosen for the experiment discussed herein.

In essence, the distributed feedback laser is a more compact version of the external cavity FBG laser discussed above (27). The usual configuration of such a device implements a standard exit reflector attached to a semiconductor photo-generating substrate. The novel feature is the integration of a Bragg grating structure as the rear reflector deposited at the other end of the semiconductor lasing cavity. The rear Bragg mirror is said to be a "distributed" reflector because reflections occur over some short thickness of the Bragg modulated substrate. Light emitted from such a device is consequently very coherent. Tuning may again be accomplished via changing the temperature of the device in order to change the period of the Bragg reflector as well as its index of refraction. Unfortunately, temperature changes over a range of about 40 degrees Celcius provide around 4nm of tuning in such a laser. Tuning the device via temperature is also relatively slow due to the high specific heat of the substrate and reflector. As one might imagine, because of the location of the substrate-deposited reflector, tuning via compressive or tensile action is impossible. Figure 8 is a schematic diagram of a DFB laser and its operation.

The Agility unit shown in the figure includes some added functionality via a distributed front reflector, an on-chip amplifier, and electro-absorption modulator.

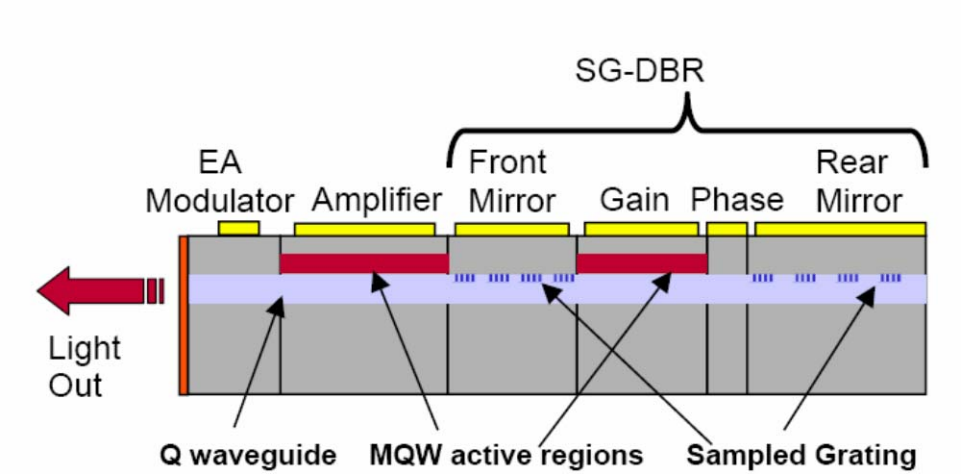

Figure 8 - DFB Laser Operation (27)

Vertical Cavity Surface Emitting Lasers are becoming increasingly prominent in optical networks and systems. Our discussion will mainly focus on MEMs based VSCELs because they are the primary focus of current VSCEL technology research. Figure 9 is a diagram of a MEMS VSCEL structure. Herein, a distributed Bragg reflector serves as the back reflector located deep within the VSCEL substrate. A quantum well active region above the substrate DBR serves as the photon source. The laser cavity is actually a 2um air gap above the substrate. The exit reflector is formed with an additional DBR suspended via a tiny single crystal semiconductor beam connected to an additional set of contacts on the substrate. Applying a voltage to the beam's contacts causes it to deflect, thus changing the cavity length and subsequently the wavelength of operation of the VSCEL. Tuning speed is relatively quick, and would make VSCELs a likely second choice for our chemical sensing application. The tuning range of a

VSCEL, which is limited primarily by the maximum deflection of the micro-beam is usually better than 20nm (28).

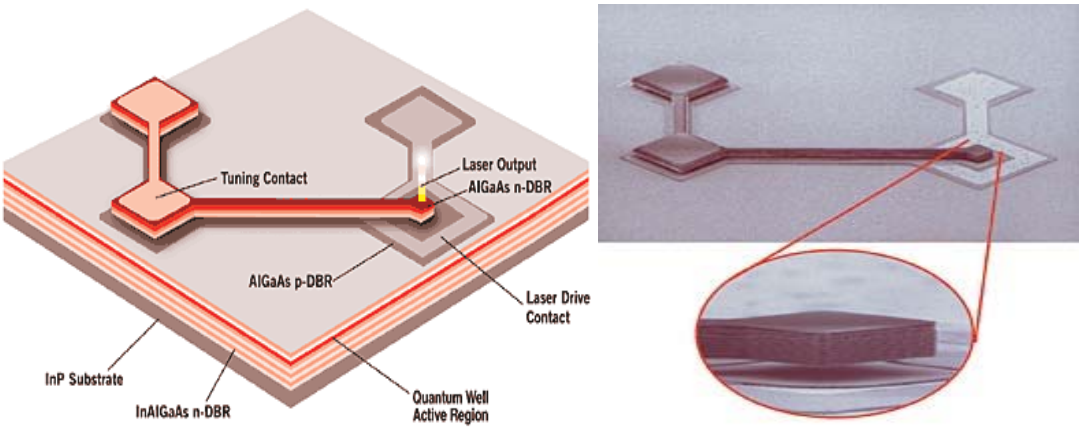

Figure 9 - MEMS Based VSCEL (28)

Only minor drawbacks exist with reference to the VSCEL. Firstly, because a crystal semiconductor is utilized to control the cavity size, some mechanical problems may arise over time altering the tuning response of the laser. In fact, with age these devices have been shown to exhibit altered wavelength/applied voltage profiles. Such effects may be compensated for by utilizing closed-loop voltage control systems. Secondly, the VSCEL has inherent limitations in output power due to the physical dimensions of the device being constrained in magnitude. In practice, an FBG laser does not necessarily have any real power limitation, save the melting or index change point of the fiber! Low-cost sensing may be effectively accomplished using VSCELs in many applications. As these devices become more readily available, it could be advantageous to attempt similar chemical sensing experimentation using a VSCEL (28).

2.6 CHEMICAL ABSORPTION

As we begin to explore the means by which the sensing of various chemical species is accomplished, we will need to understand the basic mechanisms encompassing spectroscopic absorption. Although we will by no means attempt a complicated derivation of spectroscopic principles as in a physical chemistry paper, we will attempt to offer some basis for the existence of spectral absorption lines, as well as the intensities and widths of those absorptions.

All objects in nature exhibit a distinct pattern of absorbed and reflected light, as is the basis for modern spectroscopy. The absorption pattern for every chemical compound is unique, and is a direct manifestation of the different types of bonds and electronic energy levels present in the compound. In fact, photon absorption can occur when any given electron is promoted to a different energy level in a compound. Absorptions may also occur when a molecule undergoes changes in its rotational or vibrational state. Figure 10 classifies the electromagnetic spectrum in terms of what types of excitations generally cause absorptions in a particular wavelength region. It should be noted that most near-IR transitions are a result of either changes in a molecule's vibrational state or the currently occupied state of electrons.

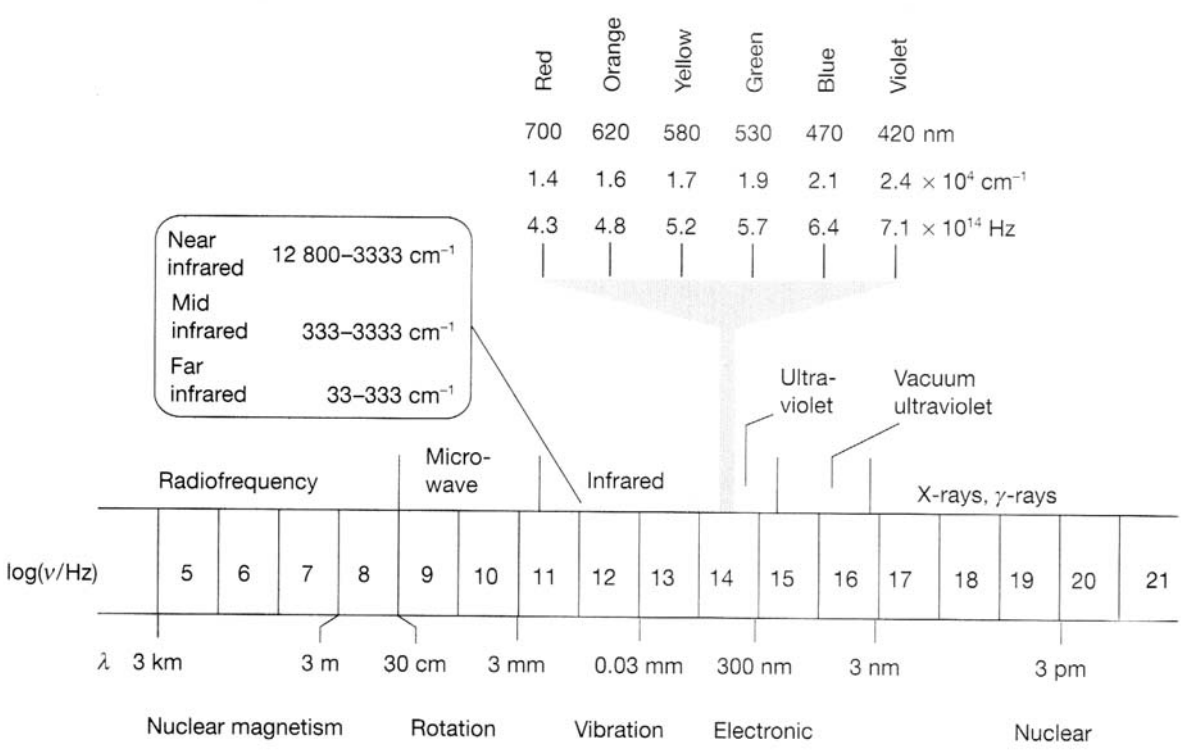

Figure 10 – Electromagnetic Spectrum Transition Origins (22)

The intensity of absorption lines has been studied extensively by spectroscopic chemists for some time. The Transmittance (T) of a sample at a given wavelength is given by:

$$T = I/I_0$$

where I is the recovered intensity and I_0 is the initially intensity of the transmitted optical beam. Empirical studies have found that recovered light intensity varies with both molar concentration (J) and sample length (L) as:

$$I = I_0 * 10^{-\varepsilon JL}$$

where ε is known as the molar absorption coefficient. Again, the molar absorption coefficient varies over frequency and is specified for particular absorption lines. As we will discuss further, the molar absorption coefficient varies widely over wavelength and may therefore not indicate the true strength of a transition at a single wavelength value. To clarify the matter, an Integrated Absorption Coefficient (A) is usually specified that accounts absorption over a small frequency range by:

$$A = \int \varepsilon(\nu) d\nu$$

For very narrow absorption line widths, it should be noted that the integrated coefficient is relatively close to the maximum value of the non-integrated coefficient (22).

Idealistically speaking, given the unitary energy conversion from absorbed photon to energy state transition, one would believe that absorption lines should occur only at a single wavelength corresponding to a particular transition. However, absorption lines observed in nature exhibit some finite line width by which photons of a short range of wavelengths are absorbed as shown in Figure 11. In a gas, this is due almost entirely to an effect known as Doppler Broadening. The cause of this phenomenon is essentially the thermal movement of molecules. As molecules in a sample move around and vibrate, they are being struck by the probing beam of photons at various angles. Some of the molecules are moving away as they are struck, and some are moving towards the photons. Thus, the observed (from the viewpoint of the molecule) frequency of photons for molecules traveling at non-relativistic speeds (s) is given approximately by:

$$\nu_{obs} \approx \nu/(1 \pm s/c).$$

The ± sign is due to the possibility that the molecule is traveling towards or away from the incident photons (c is the standard symbol for the speed of light in a vacuum).

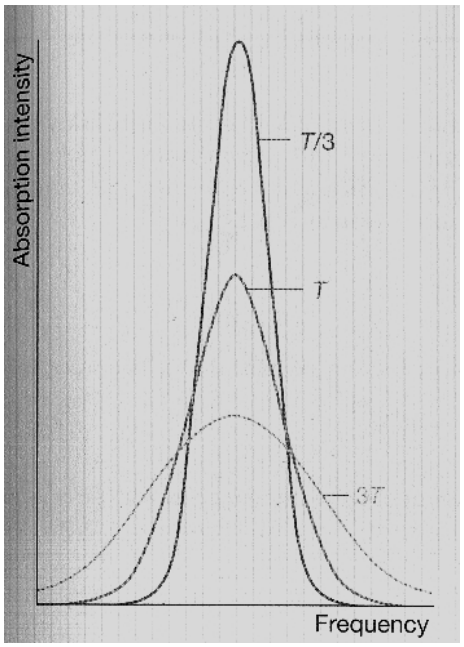

Figure 11 – Absorption Line Width for Different Temperatures (22)

The full width at half-maximum line-width for a molecular species of mass (m) at a given temperature has been derived as:

$$\delta\lambda = 2\lambda/c(2kT*\ln 2/m)^{1/2}$$

where m is the (MKS) mass of the molecule, k is Boltzman's constant, and T is the absolute temperature. One should note that the average speed of molecular movement, and therefore the line-width, is determined by temperature. In many cases, spectral measurements are taken at extremely low temperatures to ensure narrow distinct line-widths. If spectral lines are far enough apart, such measures may not be necessary for detection and analysis.

In our experiment, acetylene gas will be utilized to test the proposed measurement system. The reason for utilizing acetylene is fairly straight forward. Firstly, acetylene has a well-detailed spectrum in the near-IR range for which a number of inexpensive emitters and photo-detectors exist. Secondly, the absorption lines in acetylene are far enough apart to be distinguished from each other at room temperature and reasonable pressures. Finally, acetylene's near-IR absorption lines are significantly far enough from those of other atmospheric components like water, nitrogen, and oxygen to make measurement possible without initial high-vacuum levels. If a number of detectable gasses are compared, as in Table 1, one will note that acetylene is readily detectable with extremely high accuracy using absorption lines near 1520nm. Upon examination of this table, one will also note that there are indeed a number of other gasses that are readily detectable with absorptions in the mid-IR and near-IR range. For reference, the Table in question was constructed assuming a 1m absorption path length, $1X10^{-5}$ absorbance limit, and a minimum 1HZ bandwidth.

Table 1 - Spectroscopicaly Detectable Gasses (29)

Molecule	Symbol	Mid-Infrared		Near-Infrared	
		(ppb)	lambda (nm)	(ppb)	lambda (nm)
water	H2O	2	5940	60	1390
carbon dioxide	CO2	0.13	4230	3000	1960
carbon monoxide	CO	0.75	4600	30000	1570
				500	2330
nitric oxide	NO	5.8	5250	60000	1800
				1000	2650
nitrogen dioxide	NO2	3	6140	340	680
nitrous oxide	N2O	0.44	4470	1000	2260
sulfur dioxide	SO2	14	7280		
methane	CH4	1.7	3260	600	1650
acetylene	C2H2	3.5	7400	80	1520
hydrogen fluoride	HF			10	1310
hydrogen chloride	HCl	0.83	3400	150	1790
hydrogen bromide	HBr	7.2	3820	600	1960
hydrogen iodide	HI	2100	1540		
hydrogen cyanide	HCN	12	6910	290	1540
hydrogen sulfide	H2S			20000	1570
ozone	O3	11	9500		
ammonia	NH3	0.8	10300	800	1500
formaldehyde	H2CO	8.4	3550	50000	1930
phosphine	PH3	6.2	10100	1000	2150
oxygen	O2			78000	760

2.7 SPECTROSCOPIC MEASUREMENT

Now that a clear basis for the physical origins of chemical opto-absorption has been detailed, we may embark upon discussion of the absorption measurement technique utilized in this experiment. First, the basic methods by which second harmonic measurements are derived will be provided. Then, some discussion of the relevance of such a technique will be presented.

Second harmonic absorption measurement is a common technique used to determine gas concentrations. In essence, the technique requires that the wavelength of the probing light source be modulated about the desired absorption peak in the given test gas. Several important conditions must be met during modulation. First, the source wavelength must be increased and decreased to values above and below the absorption peak. For narrow absorption line-widths, these values could be as little as .1nm apart. Secondly, while the source wavelength is centered exactly on top of the absorption line, some light must still propagate through the sample which is still measurable by the detection circuitry. Finally, if possible, the modulation range should be centered exactly above the desired absorption peak.

During modulation, some interesting results are apparent. Each time the source wavelength is increased from its minimum, passing the absorption wavelength, and reaching its maximum; the recovered optical output "dips" from its un-absorbed maximum to some minimum value. As the source wavelength decreases again towards the minimum value, another absorption "dip" occurs. Thus, for one cycle of wavelength modulation two "dips" in the recovered output power exist. If the source is exactly centered upon a given absorption peak, the recovered signal will be a perfect sine wave whose magnitude is a direct result of the magnitude of the absorption line in the gas.

Fortunately, the second harmonic measurement technique is extremely forgiving in accuracy and clarity. There do, however, exist a number of conditions that can easily distort the recovered sinusoid in such a test. If the source wavelength range is not centered exactly upon the absorption peak, the recovered signal will appear skewed somewhat. If the modulated wavelength range is larger than necessary, the output signal will also not be perfectly sinusoidal. All of these problems can most simply be eliminated through the use of a simple band-pass filter

designed to eliminate all but the content of the recovered signal at twice the modulation frequency. As long as the wavelength range encompasses the desired absorption line entirely, filtering may be used to recover a measurable modulated signal. It is for this reason that second harmonic measurements are extremely desirable, and will be utilized for this detection experiment.

As observed in Table 1, it is possible to derive the radiation losses in the test species at a particular wavelength, and subsequently derive the detection sensitivity of the device for a particular gas. First, the type of gas measurement must be determined with respect to the pressure of the test gas (24). In our case, gasses will be measured at relatively low pressures which indicate a Lorentzian lineshape for absorption bands defined by:

$$\alpha(\omega) = \frac{\alpha_0}{[(\omega - \omega_0)/\gamma]^2 + 1}$$

where ω_0 is the line center, and γ is the linewidth (fwhm) of the spectral absorption. Thus, the recovered power in the gas cell may again be given by the Beer-Lambert Law as:

$$P_{out} = P_{in} \exp^{-\{\alpha(\omega) L\}}$$

with L indicating the length of the laser absorption path. For the case of wavelength modulation spectroscopy detection, the sensing laser signal is characterized by a time-varying wavelength defined as:

$$\omega = \omega_0 + a \cos(f t).$$

The recovered power of the second harmonic signal (B_2) may then be given by:

$$B_2 = \tfrac{2}{\pi} P_{in} \int_0^{\pi} \cos(2x) \exp\left(\frac{-D}{1 + A^2 \cos^2 x}\right) dx$$

where Pin is the power of the probing laser, A = a/γ (relative modulation amplitude), and D = $\alpha_0 L$ (peak optical depth). This is obtained via a Fourier analysis along with utilization of the orthonormal properties of sines and cosines (24).

Measuring the amplitude of the recovered second harmonic (B_2) along with knowledge of the other applicable parameters, including the modulation amplitude (a), the absorption linewidth (γ), input laser power (P_{in}), and path length (L) allows the calculation of the absorption peak (α_0); which may be used to directly relate molar concentration of the test gas.

In order to derive a theoretical sensitivity for such a measurement, one would need to first determine the minimum detectable amplitude. Theoretically speaking, this value would be determined by the amount of dark noise at the second harmonic frequency and the amount of shot noise generated in the optical detector. This noise level would then be used to determine a minimum observable recovered power signal via the sensitivity of the detector. Although shot noise is the ultimate incurable source of inaccuracy in such a detection scheme, other sources of noise originating in detector circuitry may serve to limit the mimimum detectable gas level. Still, such methods may be used to re-iterate the detection limit shown for acetylene in Table 1 indicating an 80ppb detection limit with a reasonable optical detector and a 1m path length. In our detection circuitry the pressurization characteristics of the gas chamber provided a limit on accuracy measurements, wherein the optical detection scheme exceeded externally measurable gas concentrations. In theory, the experimental setup should be capable coming within an order of magnitude of the detection limit given in Table 1 due to the chosen absorption line measured.

3.0 EXPERIMENTAL PROCEEDURES

3.1. FBG LASER FABRICATION

As would be expected, the first step in the construction of our novel gas sensing system was to fabricate an external cavity FBG laser from a commercially available In/GaAs ridge-waveguide laser with a cavity length of 300um. The unit was purchased as a special-order device from QPhotonics, LLC as P/N QFLD-1550-10AR. In order to facilitate fabrication of the external cavity Bragg grating, the laser was ordered with an anti-reflective coating on the exit facet of the waveguide instead of the standard exit reflector coating. The unit was also provided with a pigtailed 2m length of SM-28 single mode fiber.

Fortunately, fairly elaborate specifications are provided with the purchased laser diode unit, facilitating quick integration into the FBG laser system. The measured output spectrum of the laser diode without its exit reflector is shown in Figure 12. It should be noted that a distinct mode pattern is already emerging despite the lack of an exit reflector. This is probably due to inadequacy of the antireflective coating at the laser diode cavity exit. The range of output wavelengths is, however, large enough for operation over the desired tuning range.

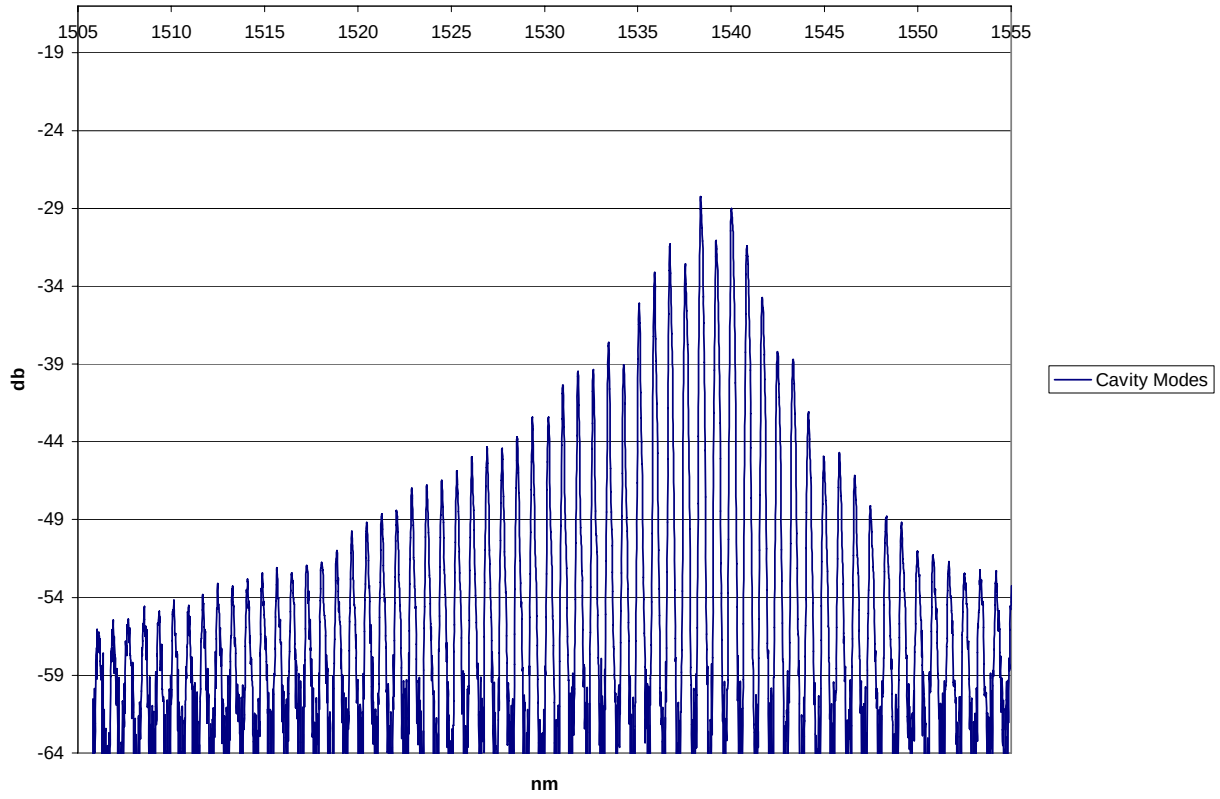

Figure 12 – Output Spectrum of Laser Diode without Exit Reflector

Detailed data is also provided regarding the laser diode's electrical operating characteristics. As indicated in Table 2, the output optical power is about 10mW; which should be enough power for lasing and subsequent sensing procedures. Figure 13 details the relationship between input current and output power, as well as junction voltage. Such a relationship is common for laser diodes of this type.

Table 2 – Laser Diode Electrical Characteristics

Parameter	Value	Units
Internal Temperature	25	°C
Thermistor Resistance	10.0	kΩ
Optical Output Power	10	mW
Threshold Current	51	mA
Operating Current	145	mA
Operating Voltage	1.76	V
Monitor Current	0.13	mA
Monitor Dark Current	0	nA
Center Wavelength	1533	nm
Spectral Width	7.48	nm

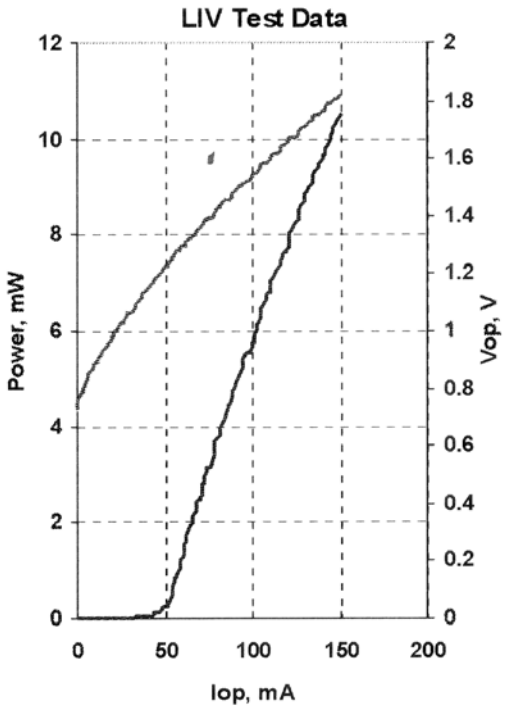

Figure 13 – Laser Diode Voltage, Current, and Output Power

The next step in producing a tunable FBG laser was to obtain an FBG and connect it to the laser diode's output fiber. Sabeus Photonics provided an FBG with a Bragg wavelength of

1529.96nm, a full-width at half-maximum bandwidth of .08nm, and a reflectivity of 50% as per our specifications. Such a wavelength was chosen to remain slightly lower than the desired absorption wavelength in acetylene gas. With subsequent up-tuning, the laser output wavelength would lie directly on top of any of the desired absorption lines. The fabricated FBG was fusion-spliced to the laser diode's output fiber using an Ericson FSU-995FA fusion splicer. The fusion splicer automatically determines the optical loss in the splice via an optical power test, which was about .07dB. The fused grating was approximately 1m from the output side of the laser diode module.

After successfully assembling the FBG laser, a suitable tuning device was constructed. Piezo-actuation was chosen as the primary means for wavelength tuning due to its accuracy in repeatability, as well as its quick actuation rate. A standard encased stack type actuator (Melles Griot 17 PAS 013) was chosen with an 80um maximum deflection at 75VDC. In this case, an actuator without feedback circuitry was chosen to simplify circuit construction. Although there is some mechanical hysteresis present in actuators of this type, it was not considered to be significant enough to merit additional feedback control for this experiment.

Special care was taken in designing a mechanism to attach the FBG to the actuator stack. The mechanism devised to marry the actuator to the fiber is shown in Figure 14. Basically, a set of mounting blocks were machined out of aluminum bar stock which were fitted to either end of the actuator. Each of these mounting blocks contained a set of 25:1 reduction worm and pinion gears with a small thumb-wheel for manual tuning input. Turning the thumb-wheel rotates an output shaft on which is mounted a 5cm diameter fiber-attachment drum. Thus, one drum is located at each end of the actuator stack with the drums being co-planar. The fiber containing

the grating was wrapped around each of the drums with the grating being centered between the two. The fiber was secured to the drum via a dab of epoxy.

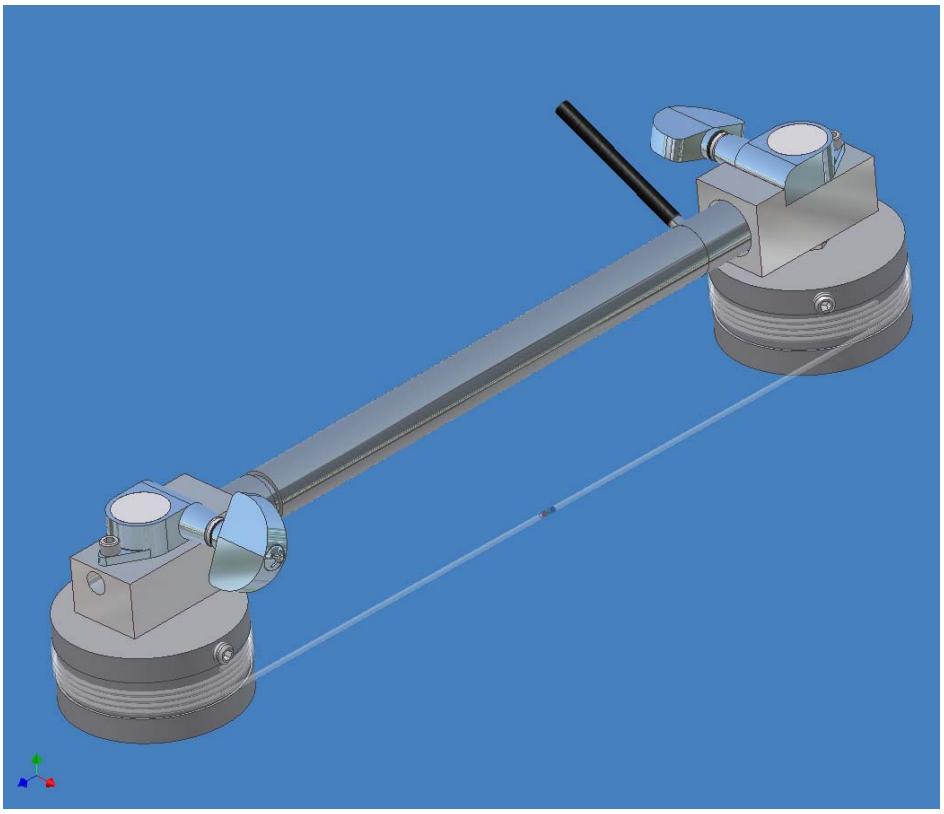

Figure 14 – Piezo-Actuator and FBG Assembly

Such construction means were implemented for several reasons. Firstly, it was necessary to attach the fiber to the actuator without clamping or distorting the fiber in any way. Doing so would have introduced significant losses and could have prevented lasing entirely. Secondly, it was necessary to maintain a baseline rest-strain in the fiber which was relatively independent of mechanical interference or "slackening" over time. The tuning drums with reduction gears described above allow stretching the FBG in the same manner that a violin string is stretched taught over the instrument's fingerboard. The friction associated with a worm and pinion gear

prevents induced rotation of the output drum, while the high gear ratio allows precise adjustment of the un-actuated strain in the fiber. In operation, one would first mechanically tune the stretching mechanism to produce laser output at roughly the correct wavelength while remaining below the exact desired output. Subsequently applying voltage to the actuator would then raise the output precisely to the desired wavelength.

In order to provide precise wavelength control for the FBG laser, an accurate, low noise high-voltage amplifier was constructed specifically for powering the laser's piezo actuator. The amplifier consisted of a +/-40V dual voltage zener-regulated power supply with 3300uf of rail to ground capacitance as well as .1uf polyester bypass capacitors on each voltage rail to provide an extremely low-ripple (<2mV) supply. The heart of the piezo-amplifier was a Burr-Brown (OPA453) 80V monolithic operational amplifier. This device has a gain-bandwidth product of about 7.5MHz and is capable of delivering a continuous 50mA to the load. The power op-amp was configured to have a DC gain of about 11. A schematic of the piezo-amplifier is shown in Figure 15. Figure 16 is a photograph of the finished unit. Therein, one should note the large rail capacitances for ripple reduction as well as the aluminum heatsink needed to cool the TO-220 monolithic op-amp.

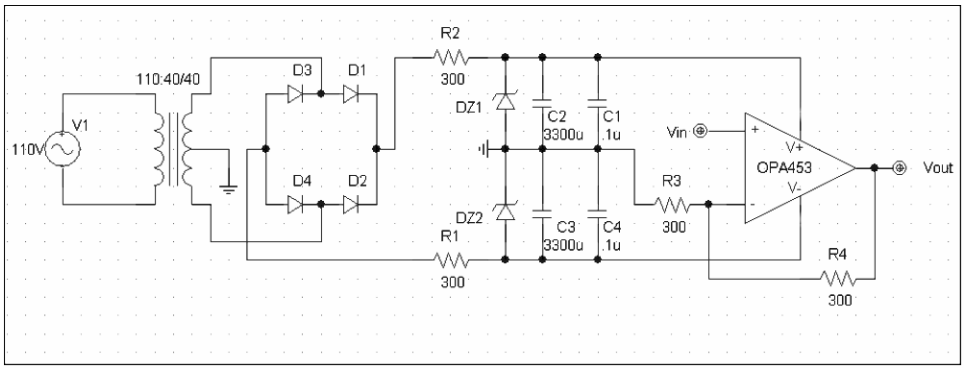

Figure 15 – Piezo-Amplifier Circuit Schematic

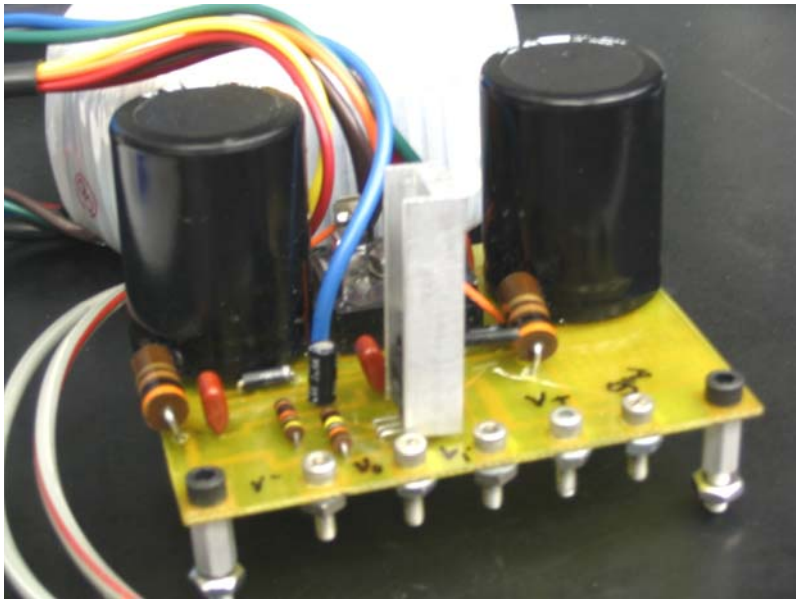

Figure 16 – Completed Piezo-Amplifier Assembly

In application of the wavelength modulation technique utilized in this experiment, it was necessary to apply an AC signal to the piezo-transducer in order to modulate the output laser wavelength. It was also necessary to apply a DC offset signal to the transducer for two reasons. Firstly, fine tuning of the laser output to a particular gaseous absorption wavelength could only be accurately accomplished via piezo-control, as manual tuning is relatively inaccurate. Secondly, if AC modulation of wavelength is to be accomplished, a DC offset level with a magnitude of at least ½ that of the peak-to-peak amplitude of the output AC sine wave needs to be applied. This is to prevent a negative polarity from being applied to the piezo-actuator, which could damage the layers of PZT material. As an additional safety measure, the negative input of the actuator was connected directly to the -40V power rail on the amplifier. The positive piezo input was subsequently connected to the op-amp output. In this manner, it was impossible to apply a reverse bias to the actuator. With zero input to the amplifier, the actuator actually

received a +40VDC bias. At the input of the amplifier, a DC power supply was connected in series with a function generator to allow for adjustment of the output DC bias as well as addition of a modulating AC signal.

After the FBG laser had been constructed, it was necessary to carefully measure the output characteristics of the device. Figure 17 shows the output spectrum of the laser in question. As shown therein, using the available mechanical and piezo-tuning devices, it was possible to tune the FBG laser over a range of more than 10nm. The far left blue trace indicates the un-stretched output while the far right green trace represents the fully stretched output. Although it may have been conceivably possible to tune the laser over a larger wavelength range, it was desirable to preserve the mechanical integrity of the fiber. Thus, the range of tuning was limited to a safe 10 nm to preserve the fiber for further experimentation.

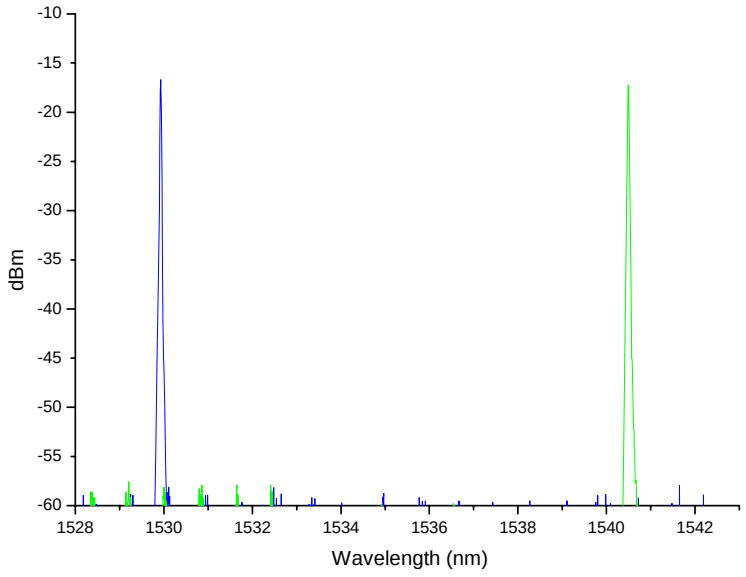

Figure 17– Laser output Spectrum (10nm mechanical tuning)

In evaluating the FBG laser, it was also necessary to determine the relationship between input current and output power. Figure 18 quantifies this characteristic. It is illustrated therein that the optical output power (integrated over the entire output spectrum) is fairly linear with respect to injection current. It can also be noted that the laser threshold current was fitted to be about 18mA with output power rising at .25uW/mA.

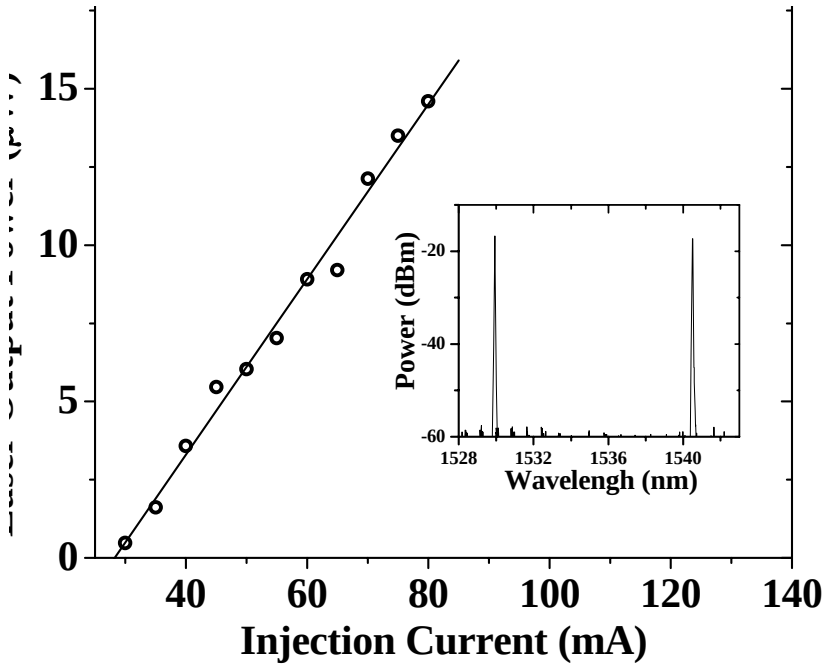

Figure 18 – Laser Output Power at Various Injection Currents

As was illustrated, the piezo-electric cell was powered via the high voltage amplifier with the capability of producing AC signals with any necessary DC offset. With such control, it was possible to obtain any base-wavelength laser output via manual mechanical stretching. A subsequently introduced DC offset allowed for fine-tuning of the output wavelength via the actuator. Finally, an AC signal generated modulation about the desired output wavelength for chemical detection. Fig. 19 is an excellent indication of the electrical tunability of the FBG laser.

It can be seen therein that the full range of movement of the piezo-actuator is capable of tuning the output laser light about 0.35nm. It is noted that the tuning rate is relatively linear. This means that an input actuator voltage translates directly to an output wavelength shift. In actuality, some mechanical hysteresis exists in the return motion of the actuator under bi-directional movement. This hysteresis can, however, be ignored over a very small range of modulation for gas species detection with narrow line widths. Simple feedback circuitry could also be utilized to linearize bi-directional movement.

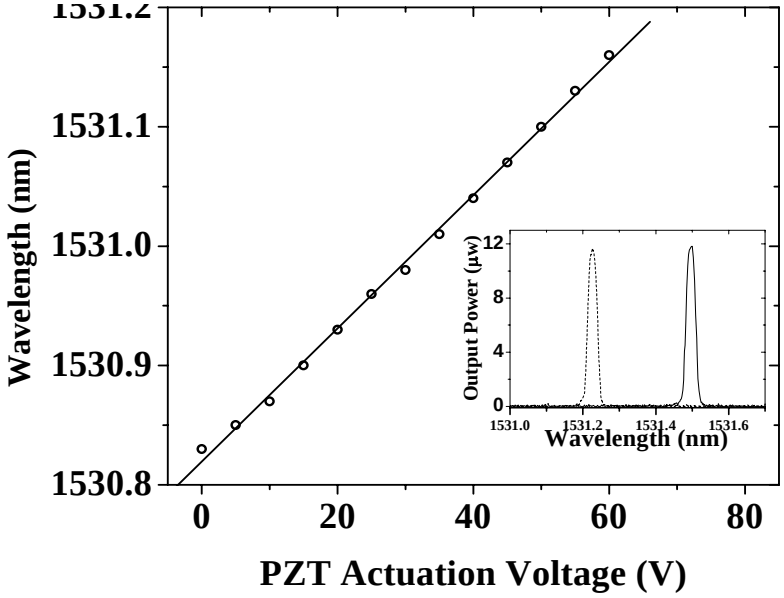

Figure 19 - FBG laser wavelength over piezo-electric input voltage. Inset – instrument limited FBG laser output spectrum with 0 and 75V actuation voltages

3.2 ABSORPTION MONITORING SETUP

Now that a suitable tunable FBG sensing laser had been constructed and evaluated, it was necessary to construct an apparatus for measuring chemical absorption in the laboratory. Such an apparatus encompassed three important systems. Firstly, optics for the transmission and recovery of the sensing laser beam through the test gas were constructed. Secondly, a vacuum system capable of delivering varying pressures of the test gas was constructed. Finally, electronic means of monitoring the returning laser beam were assembled.

It was determined that approximately one meter of transmitted laser beam would be more than sufficient to evaluate the absorptive properties of the chosen test gas; acetylene. Figure 20 diagrams the optics necessary for beam transmission and recovery. Since the FBG laser is terminated in an optical fiber, it was necessary to utilize a fiber terminated beam collimator to collimate the laser output into a parallel beam. This beam was shone through a fused silica window into the test vacuum chamber. The fused silica window served to both seal the vacuum chamber and allow the free passage of the wavelength range produced by the laser. For reference, the transmission spectrum of the fused silica windows at either end of the vacuum chamber is included in Figure 21. Therein, one will note greater than 95% transmission for wavelengths in the 1500-1600nm wavelength range.

As shown in Figure 20, upon emission from the exit side of the vacuum chamber, the sensing laser beam was recovered by a set of optical devices. To miniaturize the optical setup the exiting laser beam was routed via two >99% reflectivity mirrors thus bending the beam around a corner. The beam was then focused via a plano-convex lens with a focal length of

75mm. Near the focal point, a microscope objective was utilized to focus the recovered beam into a roughly 50um diameter beam which was then directed into an additional length of multimode fiber-optic cable for evaluation and monitoring.

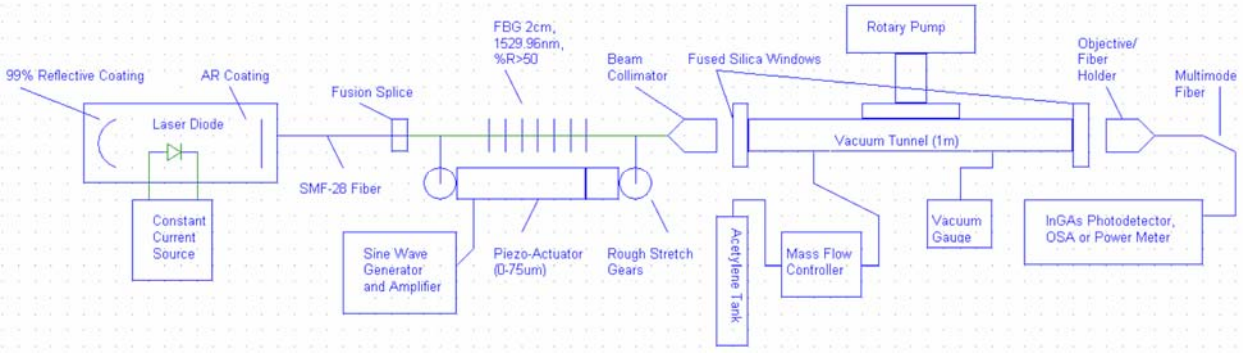

Figure 20 – Absorption Test Optics

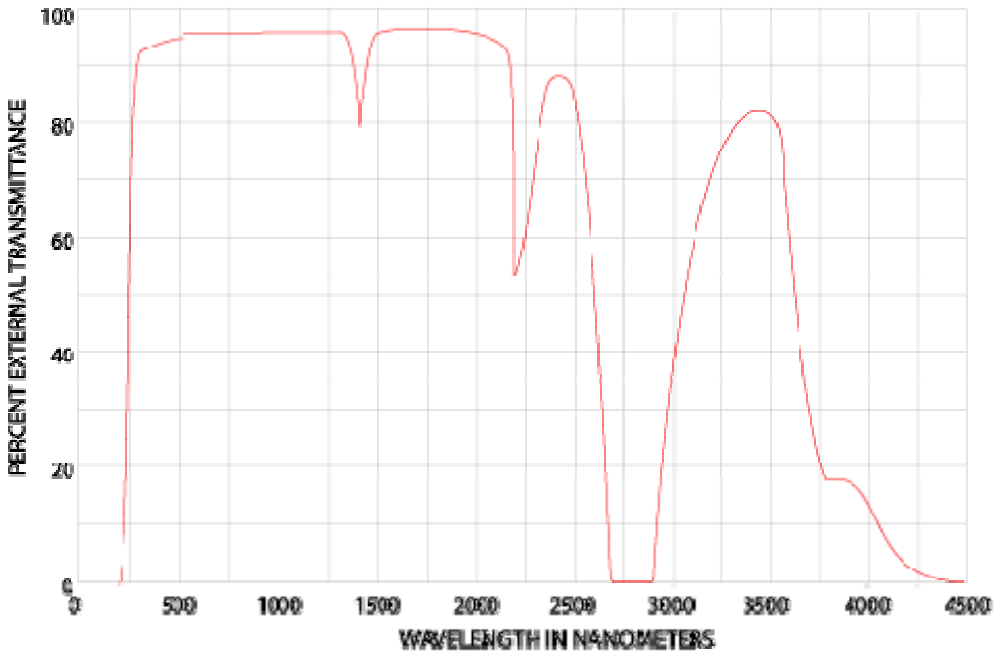

Figure 21 – Fused Silica Window Transmission Spectrum

The construction of an appropriate de-pressurization chamber was crucial to the success of the experiment in question. The chamber itself consisted of a one-meter long tunnel with the afore-mentioned fused silica windows at either end. The windows were secured with a set of compressed vacuum o-rings which were additionally sealed with vacuum grease. The center of the tunnel included an expanded section with a central access port to provide additional functionality as well as increased chamber volume for pressure stability. The entire unit was machined by the author out of cold-rolled low-carbon steel and tig-welded in-house.

A number of additional systems were required for pressure regulation and gas delivery inside the vacuum chamber. In order to provide pump-down, the chamber was fitted with an oil-free rotary-vane pump which was capable of reaching an ultimate pressure of about 100mTorr. Pressures inside the chamber were monitored with a convection style vacuum gauge rated from 1mtorr to atmosphere. Delivery of the test gas into the chamber was accomplished via a mass-flow controller fed with an acetylene tank. The mass-flow controller itself was operated via a digital control unit allowing up to 128cc/min of gas flow.

At the fiber output of the optical system devices were connected for the evaluation of gaseous absorption inside the vacuum chamber. Initially, the fiber was connected to an optical spectrum analyzer (Ando AQ6317B) for rough analysis and operational checks. Once the proper operation of the system had been determined, the output fiber was connected to an InGaAs photo-detector suitable for use in the near-infrared range. This photodiode produces a photo-current proportional to the power of the light it receives. This photocurrent was amplified and filtered with a bandpass amplifier and filter (Krohn-Hite 3500). Filtering all but twice the wavelength modulation frequency allowed observation of the second harmonic signal

apparent because of the absorption caused by the gas. The filtered photo-current signal was observed on a digital oscilloscope (HP 54603B) for measurement and storage.

4.0 EXPERIMNENTAL RESULTS

4.1 STANDARD EVALUATION

The first step in evaluating the new sensing laser was to create a standard absorption spectrum with which results obtained experimentally could be compared. The importance of doing so was primarily to pinpoint the location of the absorption lines in acetylene gas such that precise tuning for spectroscopy would be possible. It would also be pertinent to obtain the relative intensities of the various absorption lines in the spectrum in question for evaluation of spectroscopic intensity results.

In order to obtain a reference spectrum in the near-IR band for acetylene gas, a commercially available tunable laser source (Santech TSL210) was utilized. The source was connected directly to the beam collimator at the input side of the vacuum chamber. Output power was set to 2.5mW and recovered output power was measured on a spectrum analyzer (Ando AQ6317B). Acetylene partial pressure was set to 50 torr. Figure 22 shows the acetylene transmission spectrum obtained from this baseline test. It may be noted that many of the strong absorption lines appear as -70dB. This is a result of the acetylene absorbing all of the sensing light which allowed only the recovery of a noise signal. If obtaining gas concentration information were the goal, it would be necessary to either increase the incident light power or

simply measure at lower gas concentrations. The test as performed allowed the location of the strong absorption lines without regard to loss of concentration information.

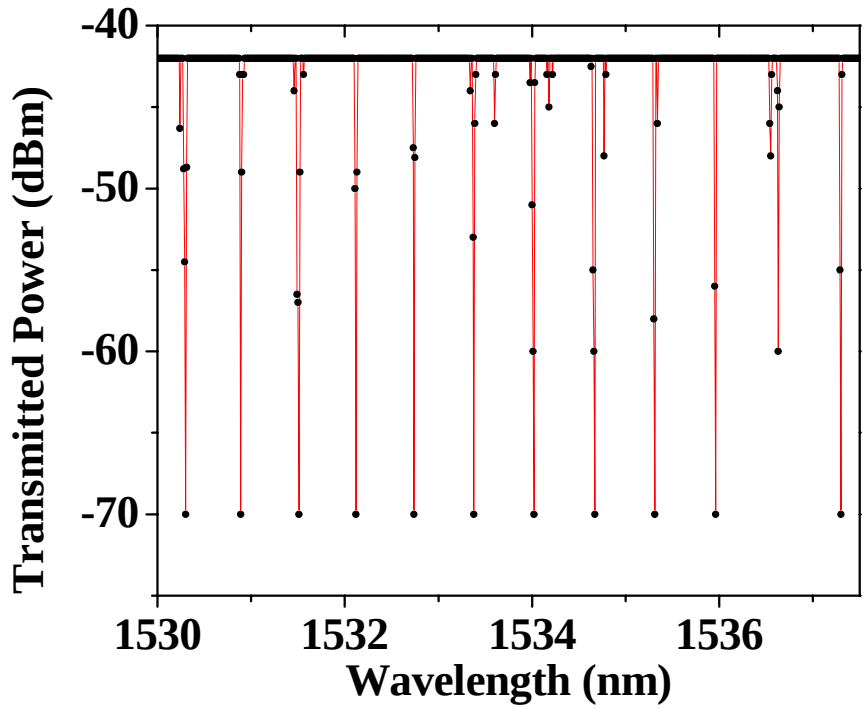

Figure 22– Baseline Acetylene Spectrum

4.2 ABSORPTION TESTING

After locating a relevant set of absorption lines using a commercial tunable laser, tests were performed using the fabricated FBG tunable laser. The first test completed involved a time-invariant test in which the tunable laser was set to a particular absorption wavelength and the pressure of the acetylene gas was varied while measuring the recovered light intensity. A second test was then performed in which the laser's output wavelength was modulated about the

absorption wavelength while measuring the amplitude of the recovered second harmonic signal via a photodetector.

Constant wavelength testing proved rather successful with the experimental setup. The FBG laser was carefully tuned to each of two clear absorption lines at 1530.9nm and 1531.5nm. Acetylene partial pressure was increased while measuring the intensity of recovered light as shown in Figure 23. Herein, the resultant plot is exceedingly linear, which was predicted for a plot which is linear in pressure and logarithmic in intensity. In this particular figure, the relative slopes of the two plots indicate the strength of the absorption lines. The steeper line corresponds to the stronger absorption.

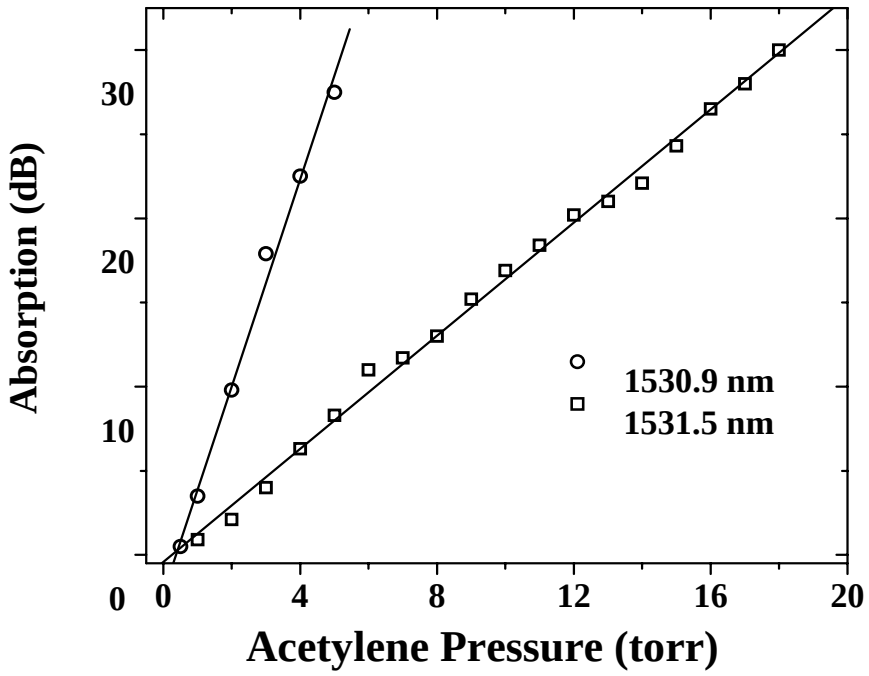

Figure 23 – Constant Wavelength Acetylene Absorption Test, Two Lines

The primary focus of this experiment was to perform the wavelength modulation procedure for which the tunable FBG laser was proponed. The laser was initially centered about each of the same two absorption lines utilized for static testing above. The piezo-actuator was then sinusoidally excited at 75Hz. This provided a 150Hz photocurrent signal proportional in magnitude to the concentration of the test gas. Figure 24 illustrates the operation of the FBG sensing system. The top plot displays the actual output voltage from the photo-detector during modulation with an acetylene pressure of 50torr. The bottom plot is the voltage applied to the piezo-actuator, while the center plot is the band-pass filtered photo-detector output.

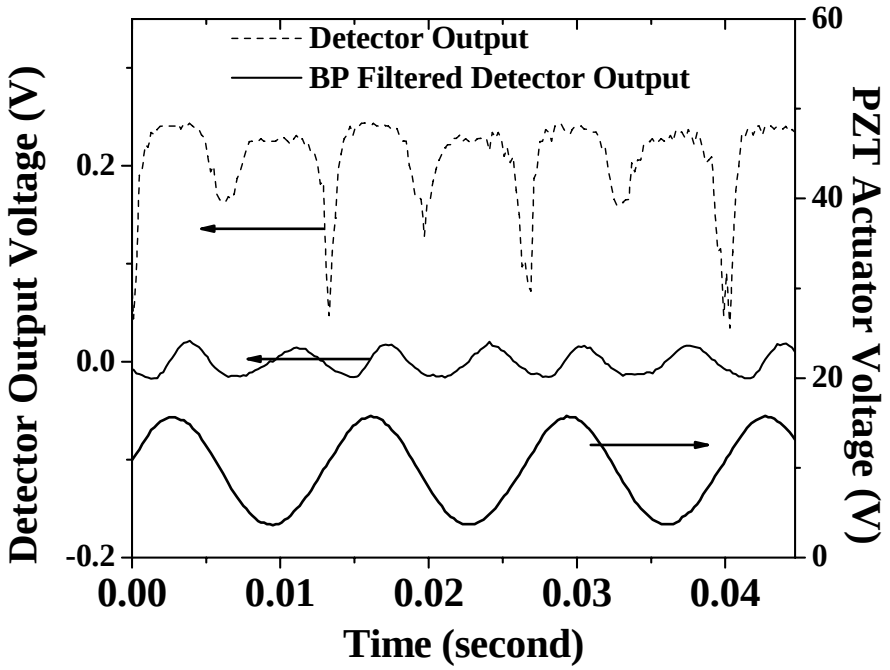

Figure 24 – Wavelength Modulation Detection

The correlation between the actuation voltage and photo detector output illustrates the operating principle behind the second harmonic recovery technique. Twice per cycle of the

actuation voltage, the output wavelength of the laser coincides with the center of the acetylene absorption line, thus causing a dip in the output photo-detector current and voltage. Ideally, the dips in the photocurrent would be equal in magnitude on either side of the peak in actuation voltage. In our case, some small deviation is present due either to some actuation hysteresis or a slightly off-centered rest wavelength. In any case, the offset is not critical enough to severely distort the filtered output voltage. One should note that the filtered version of the detector output voltage is slightly askew, but still roughly sinusoidal.

Once it was determined that a clear absorption second harmonic signal was obtainable via the experimental setup, measurements were taken at varying acetylene pressures. Figure 25 was constructed indicating the relationship between the gas pressure and second harmonic amplitude for two different absorption lines. The resulting linear relationship between pressure and amplitude was again noted. There does appear to be some variation in the measurement at 1531.5nm, possibly due to either a temperature fluctuation or some mechanical slippage in the tuning unit. Overall, it was demonstrated that gas pressures could be accurately measured in this manner to pressures as low as 200mTorr.

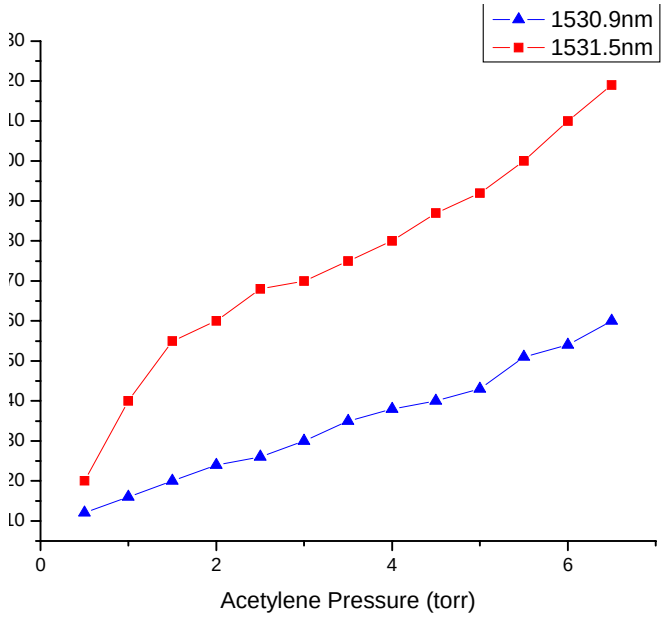

Figure 25 – Second Harmonic Amplitude with Varying Gas Pressure

5.0 ANALYSIS

5.1 SUMMARY

As we have shown, it was possible to construct a working tunable fiber Bragg grating laser and apply it to spectroscopic chemical sensing. Such an application proved rather appropriate for the FBG laser, which performed excellently in this capacity. The construction of both the tunable laser, and the accompanying chemical sensing apparatus proved to be formidable but rewarding ventures.

The tunable laser was constructed of an InGaAs ridge-waveguide with a single back reflector. The waveguide was terminated in a pigtailed single-mode fiber which was fused to a fiber Bragg grating. Tunability was accomplished via a set of tuning gears and a piezo-actuator that stretched the grating from its rest length inducing a change in the Bragg wavelength and subsequently, the lasing wavelength. Modulation was accomplished using a high voltage amplifier capable of producing AC and DC signals. Overall laser characteristics proved rather good, paving the way for subsequent absorption experimentation.

Construction of the experimental vacuum chamber and associated absorption test equipment proved also to be an arduous but successful task. The overall test chamber was a meter long with fused silica end-windows. The chamber was pumped down using a rotary vain

pump with a mass-flow controller injecting an appropriate amount of test gas. After successfully aligning the optics and de-pressurizing the chamber, gas concentrations were found to be detectable over a large range of partial pressures.

Several key concepts were discerned in the previously detailed experimentation. Firstly, the FBG laser appears to be excellently suited for gas concentration analysis. Its stability and quick tuning proved to be perfect for such a task. Secondly, gas detection required a rather complex optical and vacuum setup which incurs a good deal of cost and added size to the detection apparatus. Finally, although the second harmonic modulation technique adds some additional complexity to the design of circuitry and the laser itself, it is invaluable in simplifying the concentration measurement process.

5.2 FUTURE WORK

Although the scope of this project was rather broad and inclusive, several important steps could be taken to add to the importance of this work. Firstly, many things could be done to realize a better tunable laser, which is the heart of the sensing system. Also, a number of approaches could be taken in miniaturizing the measurement system in order to produce an extremely small and portable real-time concentration monitoring system.

Several improvements could be made to better the output characteristics of the tunable laser presented herein. Firstly, it has been shown that FBGs may be tuned up to 40nm using a slightly different tuning package than the one implemented in this experiment. Using a compressive beam structure (as described in 2.2) would effectively increase the tuning range of

the device, but may decrease the tuning speed. Some work has previously been done in which a piezo stack was bonded directly to an FBG. Such a method can also increase the tuning range somewhat over the method of simply stretching the ends of the fiber as was done here. In doing so, the strain is mitigated to the grating section of the fiber only, as opposed to an arbitrarily longer section of fiber. Finally, much can be done to improve the power output of the sensing laser; which would subsequently increase its measurement range. In one proposed design, we suggest constructing a similar sensing laser using an FBG written in multimode fiber attached to a high power (1-10w) laser diode module. Future experimentation will be required to validate the use of such a device.

Much can be said about the prospect of miniaturizing the spectroscopic system described herein. Since the sensing laser and associated electronics and power supplies are essentially easy to make very small, we must focus on the large vacuum chamber and optics which make up most of the mass of equipment. Work has recently been done using photonic crystal fibers which have air-holes built into their structure. Fibers of this nature have been used as gas-cells before, and could eventually serve as the test chamber for concentration analysis. Obviously, the difficult prospects are getting gasses in and out of the fiber, as well as achieving vacuum inside the air-gaps. If successful, such a venture could make the entirety of this measurement system fit in a small hand-held unit. It should also be noted that decreasing the chamber volume via use of a photonic crystal fiber would decrease the size of the pump needed to achieve vacuum levels. Modest miniaturization gains could also be realized via allowing the optical path inside the vacuum chamber to be reflected back and forth a number of times, thus increasing the path length several-fold. Additionally, if more sensitive circuitry were constructed for the

measurement of the second harmonic signal, optical path length could be further reduced additionally miniaturizing the device.

To be succinct, the FBG laser chemical sensing device constructed in this experiment worked every bit as well as it was expected to. Although it promises the beginnings of a compact real-time optical gas analyzer, in and of itself it is a laboratory device not intended to be extremely tiny or completely efficient. The concept of application of FBG laser technology to chemical sensing was effectively established; with experimental results adhering to theoretical expectations. The work performed here may prove to be an interesting bridge between the technologies present in the far-advanced telecommunications industry and the more primitive m jkworld of sensors and measurement. Surely, such an application brings up new prospects for sensing and novel spectroscopy techniques.

BIBLIOGRAPHY

1. Hill, K.O., et al., *Photosensitivity in optical fiber waveguides: Application to reflection filter fabrication.* Applied Physics Letters, 1978. **32**(10): p. 647-649.

2. Othonos, A. and K. Kalli, *Fiber Bragg Gratings, Fundamentals and Applications in Telecommunications and Sensing*. 1999, Norwood, USA: Artech House Publishing.

3. Inui, T., T. Komukai, and M. Nakazawa, *A wavelength-tunable dispersion equalizer using a nonlinearly chirped fiber Bragg grating pair mounted on multilayer piezoelectric transducers.* Photonics Technology Letters, IEEE, 2000. **12**(12): p. 1668-1670.

4. Song, Y.W., et al., *40-nm-wide tunable fiber ring laser with single-mode operation using a highly stretchable FBG.* Photonics Technology Letters, IEEE, 2001. **13**(11): p. 1167-1169.

5. Goh, C.S., et al., *Wavelength tuning of fiber Bragg gratings over 90 nm using a simple tuning package.* Photonics Technology Letters, IEEE, 2003. **15**(4): p. 557-559.

6. Kashyap, R., *Fiber Bragg Gratings*. 1999, San Diego, CA: Academic Press.

7. Metlz, G., W.W. Morey, and W.H. Glenn, *Formation of Bragg gratings in optical fibers by a transverse holographic method.* Optics Letters, 1989. **14**(15): p. 823-825.

8. Chen, K.P., P.R. Herman, and R. Tam, *Strong fiber Bragg grating fabrication by hybrid 157- and 248-nm laser exposure.* Photonics Technology Letters, IEEE, 2002. **14**(2): p. 170-172.

9. Atkins, R.M., V. Mizrahi, and T. Erdogan, *248 nm induced vacuum UV spectral changes in optical fibre preform cores: support for a colour centre model of photosensitivity.* Electronics Letters, 1993. **29**(4): p. 385-387.

10. Othonos, A., *Fiber Bragg gratings.* Rev. Sci. Instrum., 1997. **68**(12): p. 4309-4341.

11. Du, W., X. Tao, and H.-Y. Tam, *Temperature independent strain measurement with a fiber grating tapered cavity sensor.* Photonics Technology Letters, IEEE, 1999. **11**(5): p. 596-598.

12. Du, W.-C., X.-M. Tao, and H.-Y. Tam, *Fiber Bragg grating cavity sensor for simultaneous measurement of strain and temperature.* Photonics Technology Letters, IEEE, 1999. **11**(1): p. 105-107.

13. Malo, B., et al., *Point-by-point fabrication of micro-Bragg gratings in photosensitive fibre using single excimer pulse refractive index modification techniques.* Electronics Letters, 1993. **29**(18): p. 1668-1669.

14. Hill, K.O., et al., *Bragg gratings fabricated in monomode photosensitive optical fiber by UV exposure through a phase mask.* Applied Physics Letters, 1993. **62**(10): p. 1035-1037.

15. H. Bissessur, C. Caraglia, B. Thedrez, J.-M. Rainsant, and I. Riant, "Wavelength-versatile external fiber grating lasers for 2.5-Gb/s WDM networks," *IEEE Photon. Technol. Lett.*, vol. 11, pp. 1304–1306, Oct. 1999

16. Jun-Ichi Hashimoto, Takashi Kato, Hiromi Nakanishi, Kazunori Yoshida, Goro Sasaki, Akira Yamaguchi, Tsukuru Katsuyama, and Naoyuki Yamabayashi, "Eight-Channel Wavelength Multiplexing With 200-GHz Spacing Using Uncooled Coaxial Fiber Bragg Grating External-Cavity Semiconductor Laser Module", *IEEE Photon. Technol. Lett.*, vol. 14, no. 11, Nov. 2002.

17. Jun-Ichi Hashimoto, T. Takagi, T. Kato, G. Sasaki*, Member, IEEE*, M. Shigehara, K. Murashima, M. Shiozaki, and T. Iwashima, "Fiber-Bragg-Grating External Cavity Semiconductor Laser (FGL) Module for DWDM Transmission", *Journal of Lightwave Tech.*, vol. 21, no. 9, Sept. 2003.

18. Hong-Gang Yu, Chang-Qing Xu, Yong Wang, Jacek Wojcik, Zhi-Lin Peng, and Peter Mascher "External-Cavity Semiconductor Laser With Bragg Grating in Multimode Fiber" *IEEE Photon. Technol. Lett.*, vol. 16, no. 10, Oct. 2004.

19. A. Bergonzo, J. Jacquet, D. De Gaudemaris, J. Landreau, A. Plais, A. Vuong, H. Sillard, T. Fillion, O. Durand, H. Krol, A. Accard, and I. Riant, "Widely Vernier Tunable External Cavity Laser Including a Sampled Fiber Bragg Grating With Digital Wavelength Selection", *IEEE Photon. Technol. Lett.*, vol. 15, no. 8, Aug. 2003.

20. T. Inui, T. Komukai, and M. Nakazawa, "Highly efficient tunable fiber Bragg grating filters using multilayer piezoelectric transducers", *Optics Communications*, vol. 190, (2001)

21. Chee Goh, M.R. Mokhtar, S.A. Butler, Sze Set, Kazuro Kikuchi, and Morten Ibsen, "Wavelength Tuning of Fiber Bragg Gratings Over 90nm Using a Simple Tuning Package", *IEEE Photon. Technol. Lett.* Vol. 15, no. 4, April 2003

22. Atkins, de Paula, "Physical Chemistry", seventh edition, NY, W.H Freeman, 2002

23. B. Saleh, M. Teich, "Fundamentals of Photonics", NY, Wiley Interscience, 1991

24. K. Uehara, “Dependence of harmonic signals on sample-gas paramenters in wavelength-modulation spectroscopy for precise absorption measurements”, Appl. Phys. B. 67, 517-523,1998.

25. J.-F. Lemieux, A. Bellemare, *C.* Latrasse and M. TCtu, “Step-tunable (100GHz) hybrid laser based on Vernier effect between Fabry-Perot cavity and sampled fibre Bragg grating”, *ELECTRONICS LETTERS 27th May 1999 Vol. 35 No. 11*

26. J. da Silva, H. Kalinowski, Strain Studies in Electrical Energy TransmissionCables using an Optical Fiber Bragg Grating Sensor”, Microwave and Optoelectronics Conference, 2001, Volume 1, 6-10 Aug. 2001 Page(s):313 - 316 vol.1

27. Y. Akulova et al. “Monolithic Tunable Integrated Transmitters”, Journal of the Optical Society of America, 2005

28. Hans P. Zappe, “Optical Gas Detection with Vertical Cavity Surface Emitting Lasers”, Sensors Online, 2005

29. Southwest Sciences Website Laser Gas Sensing Tutorial, http://www.swsciences.com/technology/sensors.html, July 2005